TMEM16A contributes to oxLDL-induced macrophage foam cell formation via the p38/JNK MAPK signaling pathways

Xingfeng Chen[1], Xiaojun Wu[1], Shifan Zhang[1], Huanhao Chen[1], Yuquan Lin[1], Yusheng Peng[1], Yanhua Du[1]*, Guozheng Liang[1,2]*

[1]Department of Pharmacology, Cardiac and Cerebral Vascular Research Center, Zhongshan School of Medicine, Sun Yat-Sen University, Guangzhou, China
[2]Department of Cardiovascular Surgery of the First Affiliated Hospital and Institute for Cardiovascular Science, Suzhou Medical College, Soochow University, Suzhou, China

Submitted: 30 January 2026; **Accepted:** 9 April 2026
Online publication: 30 June 2026

Arch Med Sci
DOI: https://doi.org/10.5114/aoms/220490

***Corresponding authors:**
Yan-hua Du
Guozheng Liang
Department of Pharmacology
Zhongshan School of Medicine
Sun Yat-Sen University
74 Zhongshan 2nd Road
Guangzhou, Guangdong
510080, China
Phone: 86-20-87334787
E-mail: duyanhua@mail.sysu.edu.cn,
gliang@suda.edu.cn

Abstract

Introduction: Atherosclerotic cardiovascular disease remains the leading cause of global mortality, characterized by lipid accumulation and inflammatory cell infiltration within the arterial wall. A critical early event in atherogenesis is the formation of macrophage foam cells driven by excessive uptake of oxidized low-density lipoprotein (oxLDL). While cations such as Ca^{2+} have been extensively studied in this context, the role of Cl^- as a regulatory anion in foam cell formation remains poorly understood. The calcium-activated chloride channel TMEM16A plays an important role in many physiological processes. However, its role in macrophages remains unclear.
Material and methods: Macrophage cells were treated with oxLDL to induce foam cell formation. TMEM16A expression was modulated by siRNA-mediated knockdown or cDNA-driven overexpression, and its activity was pharmacologically inhibited using T16Ainh-A01 and CaCCinh-A01. Expression of scavenger receptor A (SR-A) and CD36, phosphorylation level of JNK, and p38 MAPK signaling pathways were analyzed by Western blotting to elucidate underlying mechanisms.
Results: OxLDL treatment significantly increased TMEM16A expression in RAW264.7 and THP-1 macrophages. Genetic silencing or pharmacological inhibition of TMEM16A markedly attenuated oxLDL-induced lipid accumulation and foam cell formation, whereas TMEM16A overexpression promoted oxLDL accumulation in macrophages. Mechanistically, TMEM16A deficiency significantly reduced SR-A and CD36 expression, which was associated with decreased phosphorylation of JNK and p38 MAPK, indicating that TMEM16A regulates SR-A and CD36 through a MAPK-dependent signaling pathway.
Conclusions: These findings demonstrate that TMEM16A plays a critical role in macrophage derived foam cell formation by promoting oxLDL uptake through activation of the JNK/p38–SR-A/CD36 axis. Targeting TMEM16A could be a promising therapeutic strategy for atherosclerosis.

Key words: chloride channel, TMEM16A, atherosclerosis, foam cells, macrophage, scavenger receptor, MAPK.

Introduction

Atherosclerosis (AS) is the pathological basis of most cardiovascular diseases and remains a leading cause of global morbidity [1]. Its primary pathological hallmark is the progressive deposition of lipids within the arterial intima, leading to luminal narrowing, loss of vascular elasticity, and, ultimately, vessel occlusion [2]. A critical initiating event during atherogenesis is the accumulation of macrophage-derived foam cells, which drive the formation of early fatty streaks and their progression into complex, chronic inflammatory lesions [3, 4].

The mechanisms underlying atherosclerosis are multifactorial, and increasing evidence suggests that dysregulated transmembrane ion transport plays an important contributory role [5]. For example, the mechanosensitive ion channel PIEZO1 mediates shear stress-induced Ca^{2+} influx, thereby linking hemodynamic cues to endothelial activation and inflammatory atherogenic responses [6, 7]. While the involvement of cations in oxidized low-density lipoprotein (oxLDL) uptake has been well characterized [8, 9], the role of anions, especially Cl^-, remains poorly understood. Chloride is the predominant extracellular anion and is essential for regulating fundamental cellular processes, including cell volume control, apoptosis and proliferation [10, 11]. Notably, recent studies have reported significant alterations in intracellular chloride concentration ($[Cl^-]_i$) in macrophages during foam cell formation, implicating chloride channels as potential regulators of lipid homeostasis [12, 13].

The calcium-activated chloride channel TMEM16A is ubiquitously expressed and has been implicated in multiple vascular pathologies, including neointima formation, cerebrovascular remodeling, and endothelial inflammation [14–16]. Our previous work demonstrated that TMEM16A regulates vascular smooth muscle cell proliferation [10, 17]; however, its specific role in macrophage lipid metabolism and atherosclerotic progression remains unclear. It has been shown to modulate macrophage foam cell formation through regulation of $[Cl^-]_i$ [12, 18, 19]; we hypothesized that TMEM16A may also act as a critical regulator of this process.

In the present study, we investigated the role of TMEM16A in oxLDL-induced macrophage foam cell formation and the underlying molecular mechanisms. Specifically, we examined whether TMEM16A promotes lipid uptake by modulating the JNK/p38 MAPK signaling pathway and the expression of SR-A and CD36. In addition, we assessed the therapeutic potential of pharmacological TMEM16A inhibition, providing a mechanistic rationale for targeting chloride channels as a novel therapeutic strategy for atherosclerosis.

Material and methods

Data availability

The data that support the findings of this study are available from the corresponding author upon reasonable request.

Preparation and oxidation of LDL

Low-density lipoproteins (LDL) were isolated from the plasma of healthy donors using sequential ultracentrifugation, as previously described [18]. Informed consent was obtained from these donors before the inclusion of the study. All donors provided informed consent, and the study protocol was approved by the Human Research Ethics Committee of Sun Yat-sen University, in accordance with the principles of the 1975 Declaration of Helsinki. Oxidized LDL (oxLDL) was generated by incubating LDL (0.2 mg protein/ml) with 5 µM Cu^{2+} in PBS at 37°C for 24 h, followed by the addition of 0.24 mM EDTA to terminate oxidation. Protein concentrations were determined using the Bradford assay with bovine serum albumin as a standard, and the extent of LDL oxidation was assessed by measuring TBARS formation. For cell culture experiments, lipoproteins were sterilized by filtration through a 0.45-µm pore filter (Millipore, Gelman Sciences, Ann Arbor, MI) and stored at 4°C in the dark until use.

Preparation of Dil-oxLDL

Native LDL was fluorescently labeled by incubation with the lipophilic dye Dil. Briefly, LDL was incubated overnight at 37°C under nitrogen protection and shielded from light, using 50 µl of Dil solution (3 mg/ml in DMSO) per milligram of LDL protein. To generate Dil-labeled oxidized LDL (Dil-oxLDL), Dil-LDL (0.1 mg/ml) was subsequently oxidized by exposure to 5 µmol/l Cu^{2+} in PBS at 37°C for 18 h in the dark. Following oxidation, excess free Dil and residual copper ions, which may cause cellular toxicity, were removed by sequential ultracentrifugation and extensive dialysis against PBS containing 0.24 mmol/l EDTA.

Cell culture and foam cell formation

Macrophage-derived foam cells were generated following an established protocol [19]. RAW264.7 murine macrophages and THP-1 human macrophages (American Type Culture Collection, Rockville, MD, USA) were cultured in RPMI 1640 medium supplemented with 10% fetal calf serum and maintained at 37°C in a humidified incubator containing 5% CO_2. To assess the temporal effects of oxidized LDL on foam cell formation, macrophages were exposed to oxLDL (80 µg/ml) for 24 h. In pharmacological TMEM16A inhibition experiments, cells were pre-treated with the

TMEM16A inhibitor T16Ainh-A01 (10 μM) or CaCCinh-A01 (30 μM) for 2 h prior to oxLDL exposure. DMSO was used as a vehicle control. The concentrations of TMEM16A inhibitors were chosen based on prior literature [20, 21] and our preliminary dose-response experiments in macrophages. Foam cell formation was subsequently assessed by visualization of lipid accumulation using Oil Red O staining (Sigma Aldrich, USA).

Uptake of oxLDL

To assess the involvement of TMEM16A in receptor-dependent oxLDL internalization, Dil-oxLDL was employed according to established protocols [22, 23]. To evaluate oxLDL uptake, RAW264.7 macrophages were incubated with Dil-oxLDL (30 μg/ml) at 37°C for 6 h. Following incubation, intracellular fluorescence was visualized using confocal microscopy with a 40× objective. For quantitative analysis, fluorescence intensity was measured in five randomly selected fields per sample, and mean cellular fluorescence was calculated using Fluoview image analysis software.

TMEM16A overexpression and knockdown in macrophages

For TMEM16A overexpression, adenoviruses carrying TMEM16A cDNA were designed and produced by Obio Technology (Shanghai, China). The cultured RAW264.7 macrophages at 70% confluence were infected with Ad-TMEM16A (100 MOI) or Ad-RFP vector control for 6 h, and then cells were washed and incubated in fresh medium for 48 h before experimentation. After that, TMEM16A protein expression was verified by Western blotting.

For gene silencing experiments, small interfering RNA (siRNA) targeting mouse *Tmem16a* (5′-CUGCUCAAGUUUGUGAACUTT-3′) and a non-targeting scrambled control siRNA were synthesized by Obio Technology (Shanghai, China). RAW264.7 cells were seeded in 6-well plates at a density of 5×10^5 cells/ml in Opti-MEM medium and transfected using HiPerFect transfection reagent according to the manufacturer's instructions. siRNA and HiPerFect were diluted separately in serum-free medium, mixed, and incubated for 20 min at room temperature before being added to the cells, yielding a final siRNA concentration of 40 nM. Cells were incubated for 48 h, after which knockdown efficiency was assessed by Western blot analysis of TMEM16A protein levels.

To examine the functional effects of TMEM16A overexpression or knockdown on foam cell formation, oxLDL was added to the culture medium at a final concentration of 80 μg/ml following completion of Ad-TMEM16A or siRNA transfection. Cells were subsequently incubated for an additional 6–48 h under standard culture conditions prior to downstream analyses.

Western blot

OxLDL-treated RAW264.7-derived foam cells were washed with ice-cold phosphate-buffered saline (PBS) and lysed in RIPA buffer supplemented with a protease inhibitor cocktail (Merck, Germany). Total protein concentrations were quantified using a bicinchoninic acid (BCA) assay. Equal amounts of protein (80 μg) were denatured by boiling for 10 min in SDS sample buffer containing 2% SDS and 2-mercaptoethanol, resolved on 10% SDS–polyacrylamide gels, and transferred onto polyvinylidene fluoride (PVDF) membranes (Millipore, USA). Membranes were blocked with 5% non-fat milk prepared in Tris-buffered saline containing 0.1% Tween-20 (TBST; 20 mM Tris–HCl, 150 mM NaCl, pH 7.5) for 1 h at room temperature, followed by overnight incubation at 4°C with primary antibodies against SR-A (1 : 1000; Abcam), CD36 (1 : 1000; Proteintech), JNK, p-JNK, p38 and phospho-p38 (1 : 1000; Cell Signaling Technology). After washing, membranes were incubated with horseradish peroxidase–conjugated secondary antibodies (1 : 1000; Cell Signaling Technology) for 1 h at room temperature. β-Actin and α-tubulin (1 : 1000; Santa Cruz Biotechnology) were used as loading controls. Protein bands were visualized using enhanced chemiluminescence (ECL) reagents (Pierce, Thermo Scientific) and quantified by densitometric analysis with a computer-assisted one-dimensional gel analysis system.

Statistical analysis

Data are presented as mean ± SEM. All datasets were tested for normality using the Shapiro-Wilk test and confirmed to be normally distributed. Differences were analyzed by an unpaired 2-tailed Student *t* test or one-way analysis of variance (ANOVA) followed by a Bonferroni multiple comparison post-hoc test. $P < 0.05$ was considered statistically significant.

Results

TMEM16A promotes oxLDL-induced macrophage foam cell formation

To determine whether TMEM16A is involved in macrophage foam cell formation, RAW264.7 macrophages were treated with oxidized low-density lipoprotein (oxLDL). Oil Red O staining demonstrated that oxLDL treatment (80 μg/ml) markedly induced intracellular lipid droplet accumulation after 24 h, indicating robust foam cell formation compared with untreated controls (Figure 1 A).

Quantitative analysis confirmed a significant increase in Oil Red O staining intensity following ox-LDL exposure. In parallel with lipid accumulation, TMEM16A protein expression was significantly upregulated in RAW264.7 cells after oxLDL stimulation (Figure 1 B). These findings indicate a close association between TMEM16A expression and foam cell formation.

To assess whether TMEM16A directly contributes to oxLDL-induced foam cell formation,

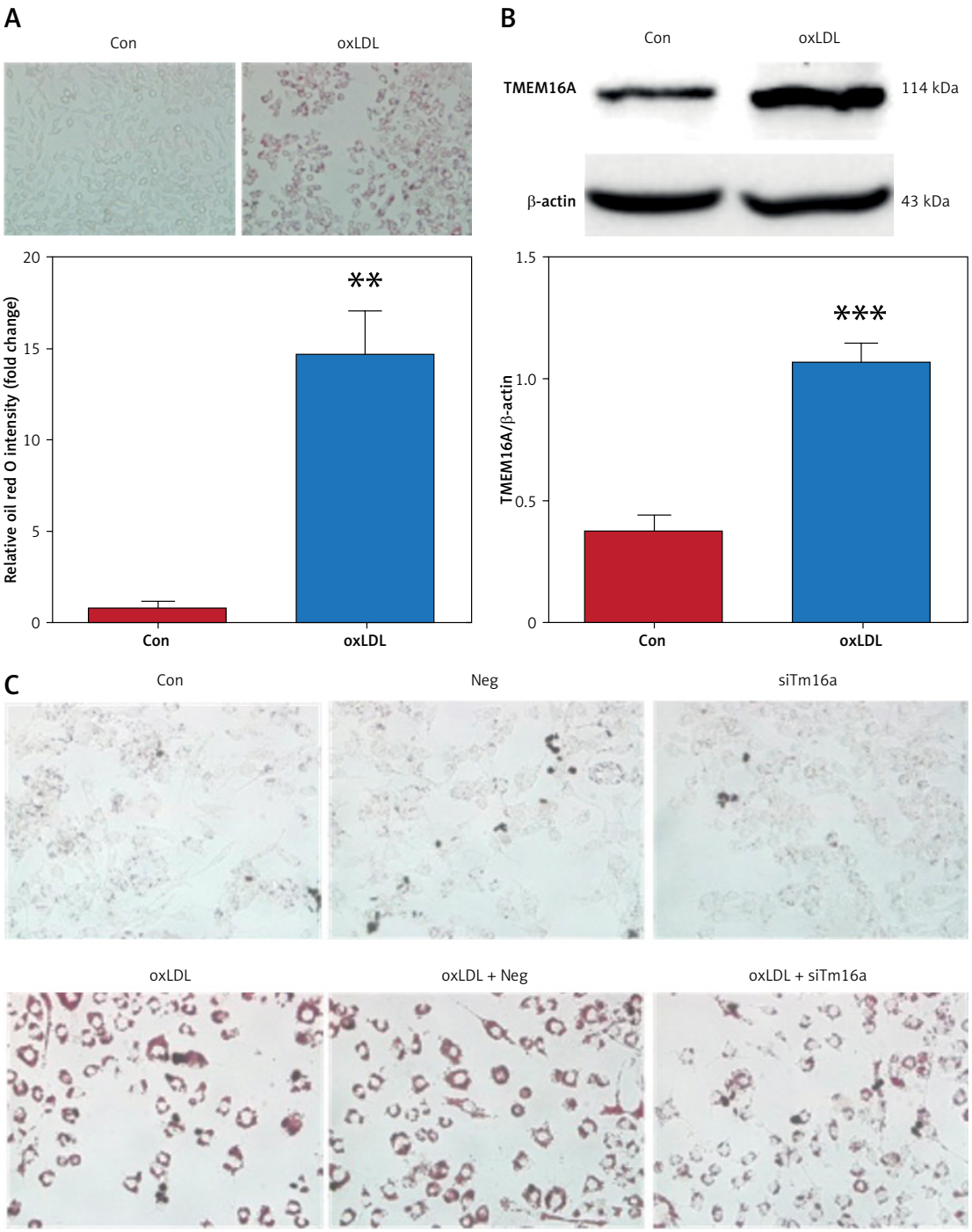

Figure 1. OxLDL induced macrophage-derived foam cell formation by increasing TMEM16A expression. **A** – RAW264.7 cells were treated with or without 80 μg/ml oxLDL for 24 h, then were stained with 0.3% Oil Red O. Images showing foam cell formation were taken under a microscope at 400× magnification (n = 3, $^{**}p < 0.01$ vs. Con). **B** – Expression of TMEM16A protein during the process of foam cell formation (n = 6, $^{***}p < 0.001$ vs. Con). **C** – RAW264.7 cells were transfected by TMEM16A siRNA (siRNA) with 40 nM concentration for 48 h. Then cells were treated with or without 80 μg/ml oxLDL for 24 h and stained with Oil Red O. Images showing foam cell formation were taken under a microscope at 400× magnification (n = 4, $^{***}p < 0.001$ vs. Neg; $^{###}p < 0.001$ vs oxLDL+ Neg)

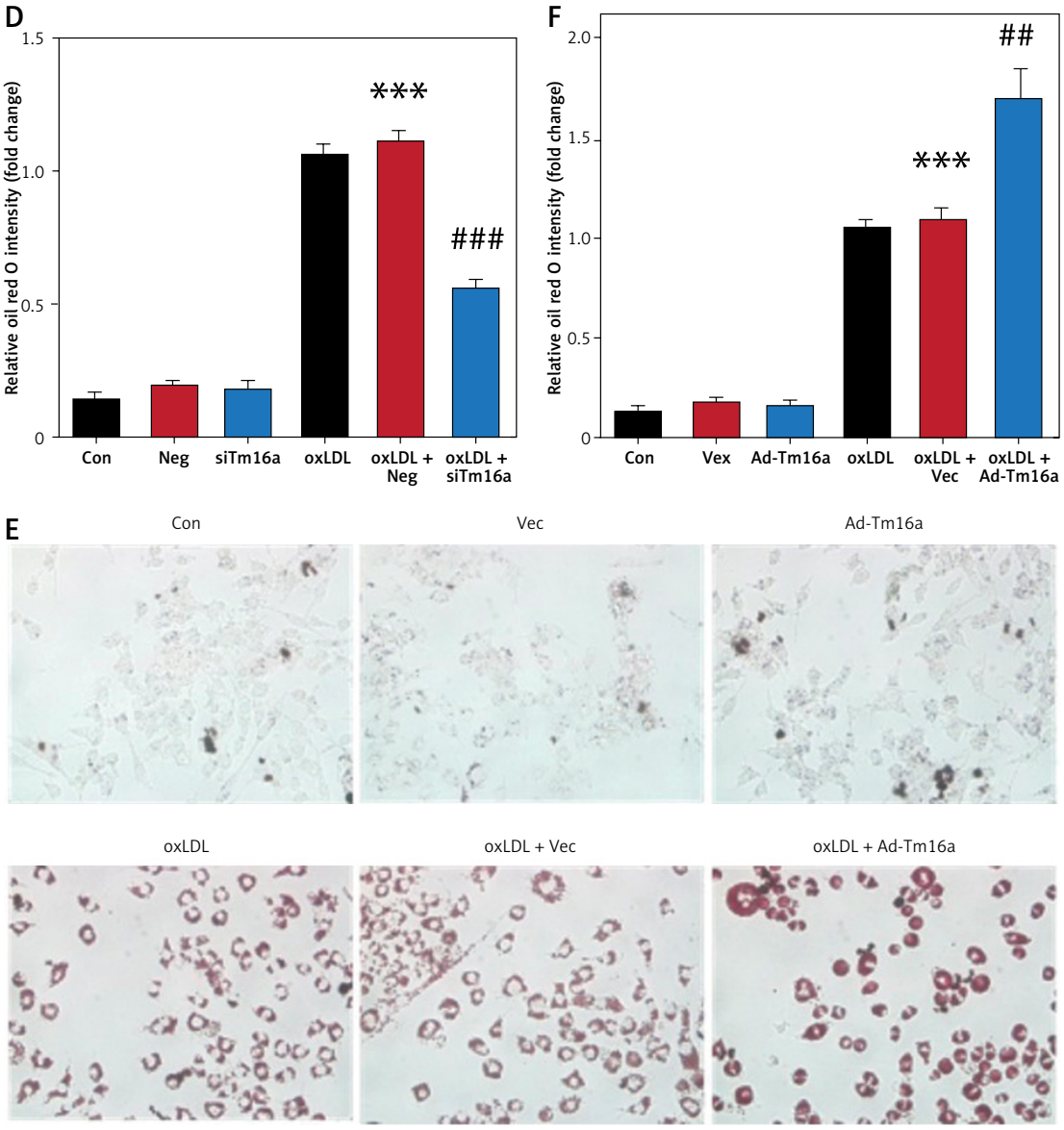

Figure 1. Cont. **D** – RAW264.7 cells were transfected by TMEM16A siRNA (siRNA) with 40 nM concentration for 48 h. Then cells were treated with or without 80 μg/ml oxLDL for 24 h and stained with Oil Red O. Images showing foam cell formation were taken under a microscope at 400× magnification (n = 4, ***p < 0.001 vs. Neg; ###p < 0.001 vs oxLDL+ Neg). **E**, **F** – RAW264.7 cells were transfected by adenovirus carrying TMEM16A cDNA (Ad-TM16A) or vector (Vec) with 100 MOI concentration for 48 h. Then cells were treated with or without 80 μg/ml oxLDL for 24 h and were stained with Oil Red O. Images showing foam cell formation were taken under a microscope at 400× magnification (n = 4, ***p < 0.001 vs. Vec; ##p < 0.01 vs oxLDL+ Vec)

TMEM16A expression was manipulated using siRNA-mediated knockdown or adenoviral overexpression (Supplementary Figure S1). TMEM16A silencing significantly reduced oxLDL-induced lipid accumulation, as evidenced by decreased Oil Red O staining (Figures 1 C, D). In contrast, TMEM16A overexpression markedly enhanced oxLDL-induced foam cell formation (Figures 1 E, F). Together, these data indicate that TMEM16A is not only upregulated by oxLDL but also functionally promotes macrophage foam cell formation.

TMEM16A enhances oxLDL uptake and promotes SR-A/CD36 expression

Macrophage foam cell formation depends on scavenger receptor–mediated uptake of oxLDL. SR-A and CD36 are the primary receptors for oxLDL uptake [24]. Dil-oxLDL fluorescence assays revealed that TMEM16A silencing significantly reduced oxLDL uptake, while TMEM16A overexpression significantly increased intracellular Dil-oxLDL fluorescence intensity (Figures 2 A–D). Consistently, Western blot analysis showed that oxLDL stimulation significantly increased the protein expres-

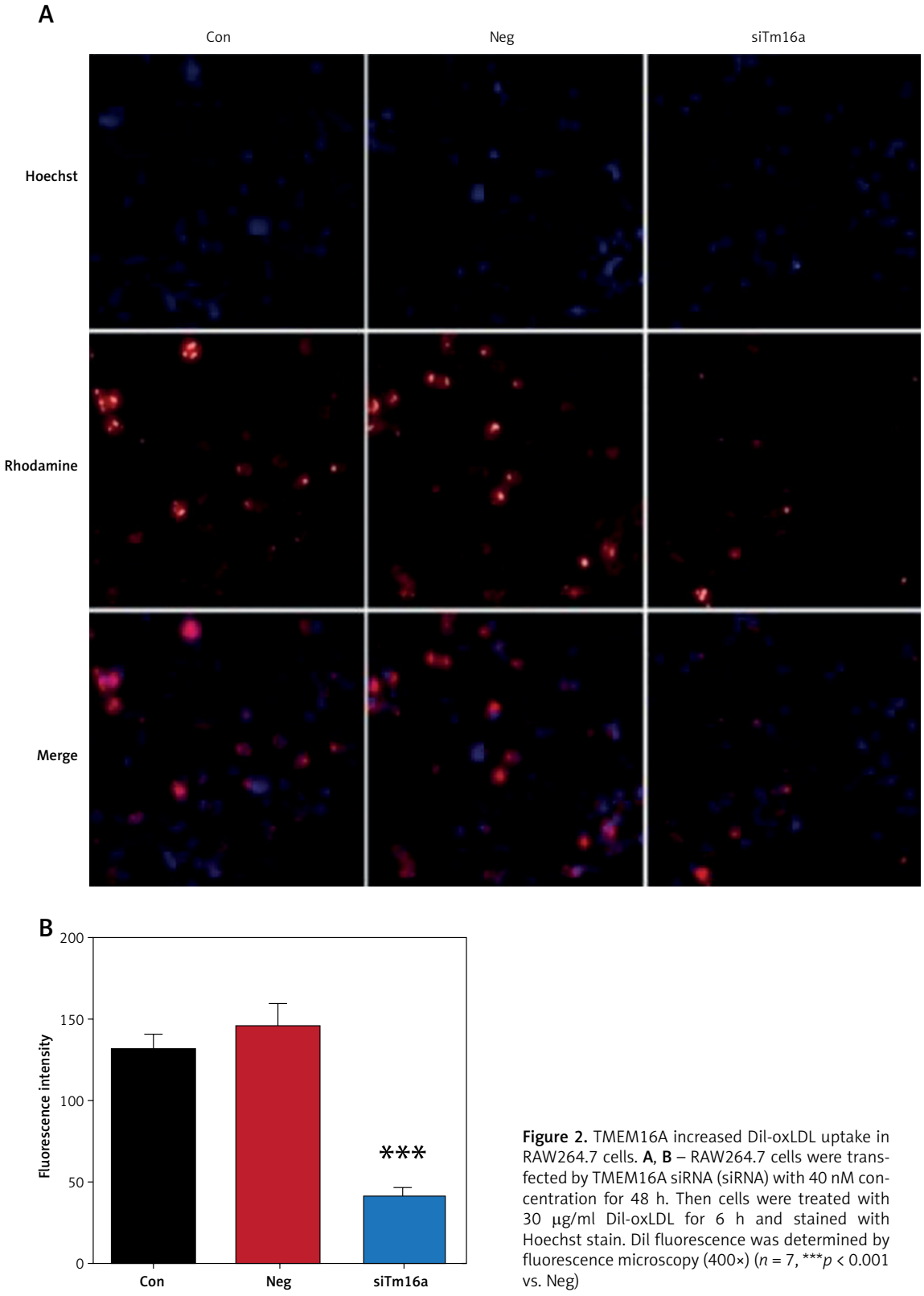

Figure 2. TMEM16A increased Dil-oxLDL uptake in RAW264.7 cells. **A**, **B** – RAW264.7 cells were transfected by TMEM16A siRNA (siRNA) with 40 nM concentration for 48 h. Then cells were treated with 30 μg/ml Dil-oxLDL for 6 h and stained with Hoechst stain. Dil fluorescence was determined by fluorescence microscopy (400×) (n = 7, ***p < 0.001 vs. Neg)

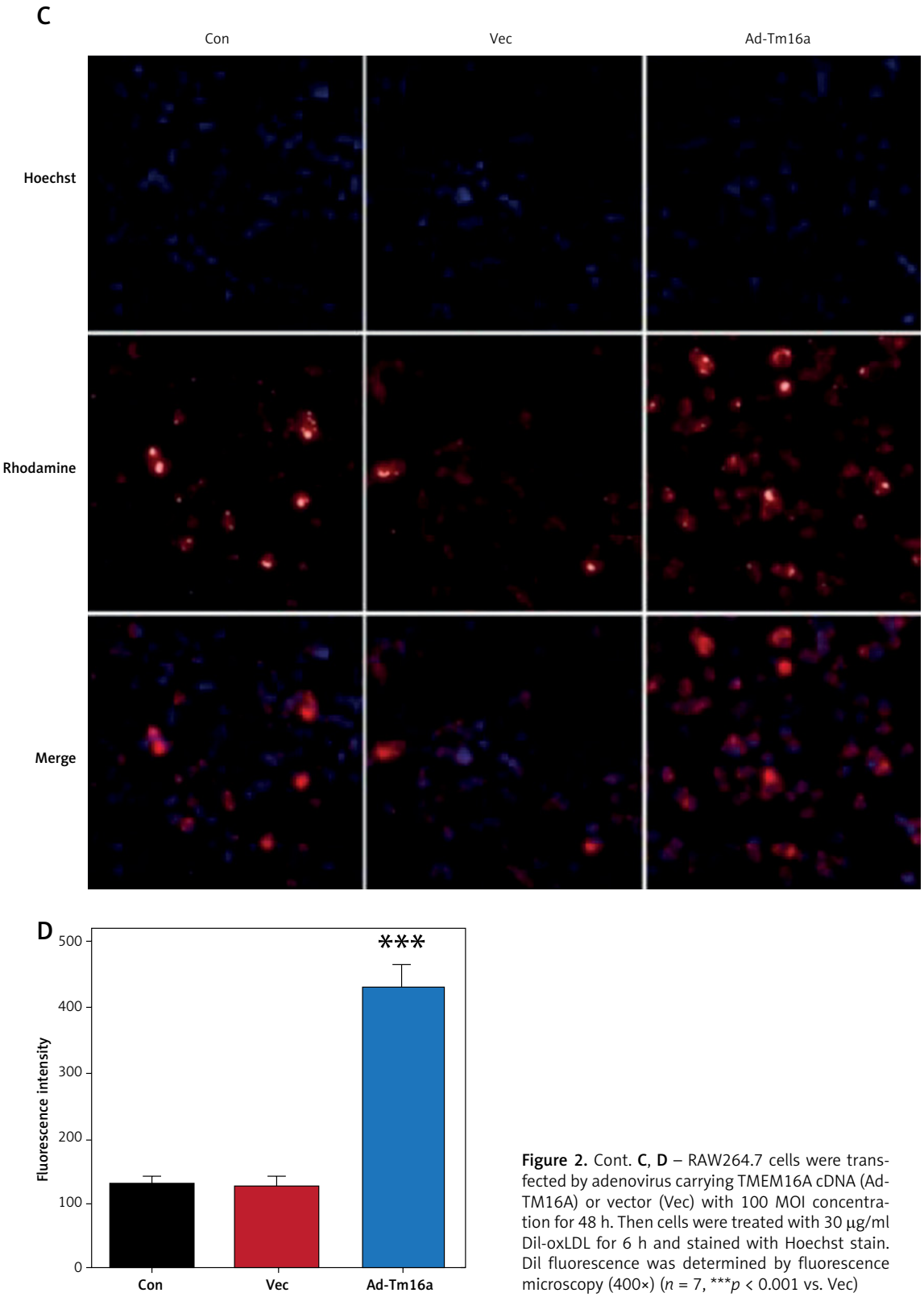

Figure 2. Cont. **C**, **D** – RAW264.7 cells were transfected by adenovirus carrying TMEM16A cDNA (Ad-TM16A) or vector (Vec) with 100 MOI concentration for 48 h. Then cells were treated with 30 μg/ml Dil-oxLDL for 6 h and stained with Hoechst stain. Dil fluorescence was determined by fluorescence microscopy (400×) (n = 7, ***p < 0.001 vs. Vec)

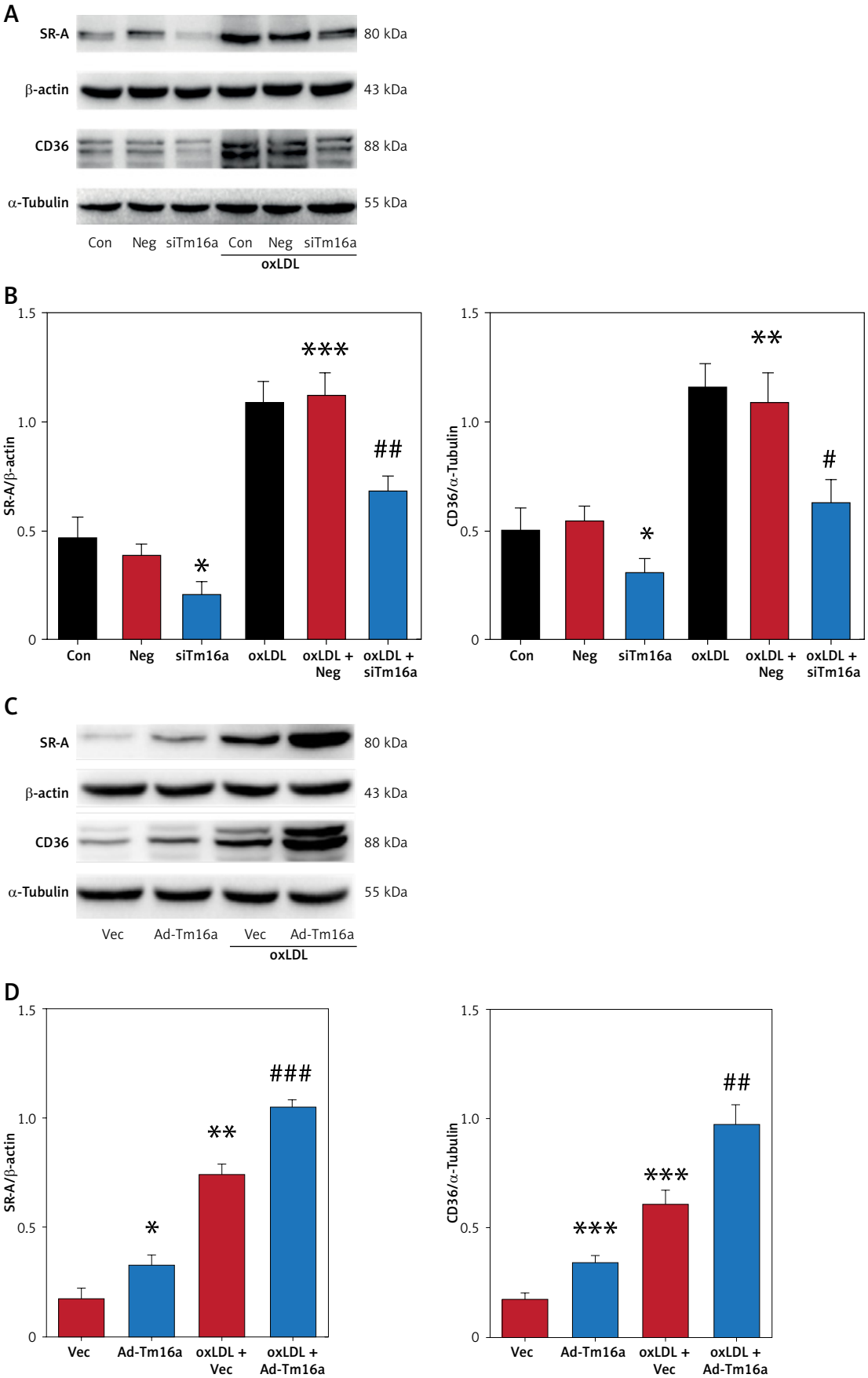

Figure 3. TMEM16A regulates expression of SR-A and CD36 in RAW264.7 cells. **A**, **B** – RAW264.7 cells were transfected by TMEM16A siRNA (siRNA) with 40 nM concentration for 48 h. Then cells were treated with or without 80 μg/ml oxLDL for 24 h. Western blot was used to detect the expression of SR-A and CD36 (n = 5, *p < 0.05, **p < 0.01, ***p < 0.001 vs. Neg; $^{\#}p$ < 0.05, $^{\#\#}p$ < 0.01 vs. oxLDL + Neg). C and D, RAW264.7 cells were transfected by adenovirus carrying TMEM16A cDNA (Ad-TM16A) or vector (Vec) with 100 MOI concentration for 48 h. Then cells were treated with or without 80 μg/ml oxLDL for 24 h. Western blot was used to detect the expression of SR-A and CD36 (n = 5, *p < 0.05, ***p < 0.001 vs. Vec; $^{\#\#}p$ < 0.01, $^{\#\#\#}p$ < 0.001 vs. oxLDL + Vec)

sion of SR-A and CD36 in RAW264.7 macrophages. Notably, TMEM16A knockdown markedly attenuated oxLDL-induced SR-A and CD36 expression, whereas TMEM16A overexpression further enhanced the expression of both receptors (Figures 3 A–D). These results demonstrate that TMEM16A facilitates macrophage foam cell formation by upregulating SR-A and CD36 expression, thereby enhancing oxLDL uptake.

TMEM16A activates p38 and JNK MAPK signaling pathways

To elucidate the signaling mechanisms underlying TMEM16A-mediated regulation of scavenger receptors, we examined the activation of the JNK and p38 MAPK pathways, which are known to regulate SR-A and CD36 expression [25, 26]. OxLDL treatment markedly induced the phosphorylation of JNK and p38 MAPK in RAW264.7 macrophages. In contrast, TMEM16A knockdown significantly suppressed the phosphorylation of these two kinases under both basal and oxLDL-stimulated conditions, with no discernible effect on their total protein levels (Figures 4 A–D). Conversely, TMEM16A overexpression further enhanced JNK and p38 phosphorylation in response to oxLDL stimulation (Figures 4 E–H). These data indicate that TMEM16A acts upstream of the JNK/p38 MAPK signaling cascade and positively regulates oxLDL-induced MAPK activation in macrophages.

Pharmacological inhibition of TMEM16A prevents foam cell formation via JNK/p38–SR-A/CD36 signaling

To further validate the therapeutic potential of TMEM16A and clarify whether its functional importance is dependent on channel activity, pharmacological inhibition experiments were performed using the specific TMEM16A inhibitors T16A-A01 [27] and CaCC-A01 [28]. Pretreatment with either inhibitor significantly reduced oxLDL-induced foam cell formation, as demonstrated by Oil Red O staining and quantitative lipid analysis in RAW264.7 cells (Figures 5 A–D). Consistent with these findings, T16Ainh-A01 and CaCCinh-A01 markedly suppressed Dil-oxLDL uptake (Figures 6 A–D) and significantly reduced the protein expression of SR-A and CD36 following oxLDL stimulation (Figures 7 A–E). Moreover, pharmacological inhibition of TMEM16A effectively blocked oxLDL-induced phosphorylation of JNK and p38 MAPK (Figures 7 F–I), confirming that TMEM16A channel activity is required for activation of this signaling pathway.

Furthermore, these results were consistently recapitulated in human THP-1 macrophages. Treatment with oxLDL significantly induced THP-1 derived foam cell formation and markedly increased the protein expression of TMEM16A (Supplementary Figure S2), while TMEM16A inhibitor treatment blocked foam cell formation (Figures 8 A–D), reduced oxLDL uptake (Figures 9 A–D) and suppressed the JNK/p38–SR-A/CD36 signaling pathway (Figures 10 A–I). Collectively, pharmacological inhibition of TMEM16A effectively disrupts this signaling axis and prevents foam cell formation *in vitro*. These data demonstrate that pharmacological targeting of TMEM16A is a viable strategy to disrupt the pathological signaling that drives macrophage foam cell formation.

Discussion

In this present study, we identified a signaling axis in which TMEM16A promotes foam cell formation by activating the JNK/p38 MAPK pathway and upregulating the scavenger receptors SR-A and CD36. These findings broaden current understanding of ionic regulation in macrophages and highlight calcium-activated chloride channel TMEM16A as a key driver and promising therapeutic target of atherosclerosis.

Atherosclerosis is a chronic inflammatory disorder driven by lipid accumulation and immune cell activation within the arterial wall [29, 30], and increasing evidence indicates that inflammatory signaling and oxidative stress play central roles in the initiation and progression of atherosclerotic lesions [31]. Foam cell formation is a critical initiating event in atherogenesis and depends on the excessive uptake of oxLDL [32, 33]. Although calcium signaling and oxidative stress have been extensively studied in this context, the contribution of chloride channels, particularly TMEM16A, has remained largely unexplored [7, 34, 35]. Our data show that TMEM16A expression is markedly induced by oxLDL. Furthermore, overexpression of TMEM16A enhanced oxLDL uptake and intracellular lipid deposition, whereas genetic silencing or pharmacological inhibition of TMEM16A using T16Ainh-A01 or CaCCinh-A01 significantly attenuated foam cell formation. These findings suggest that TMEM16A-mediated chloride efflux represents an early cellular response to lipid stress in macrophages.

A key mechanistic insight from this study is that TMEM16A deficiency markedly reduced the expression of both SR-A and CD36, the two principal receptors responsible for macrophage oxLDL binding and uptake [24]. By simultaneously regulating both receptors, TMEM16A appears to function as a central upstream modulator of scavenger receptor expression rather than acting on a single downstream pathway. This dual regulation provides a robust explanation for the pronounced reduction in lipid loading observed upon TMEM16A inhibition. To define the signaling mechanism linking TMEM16A to scavenger receptor expression, we

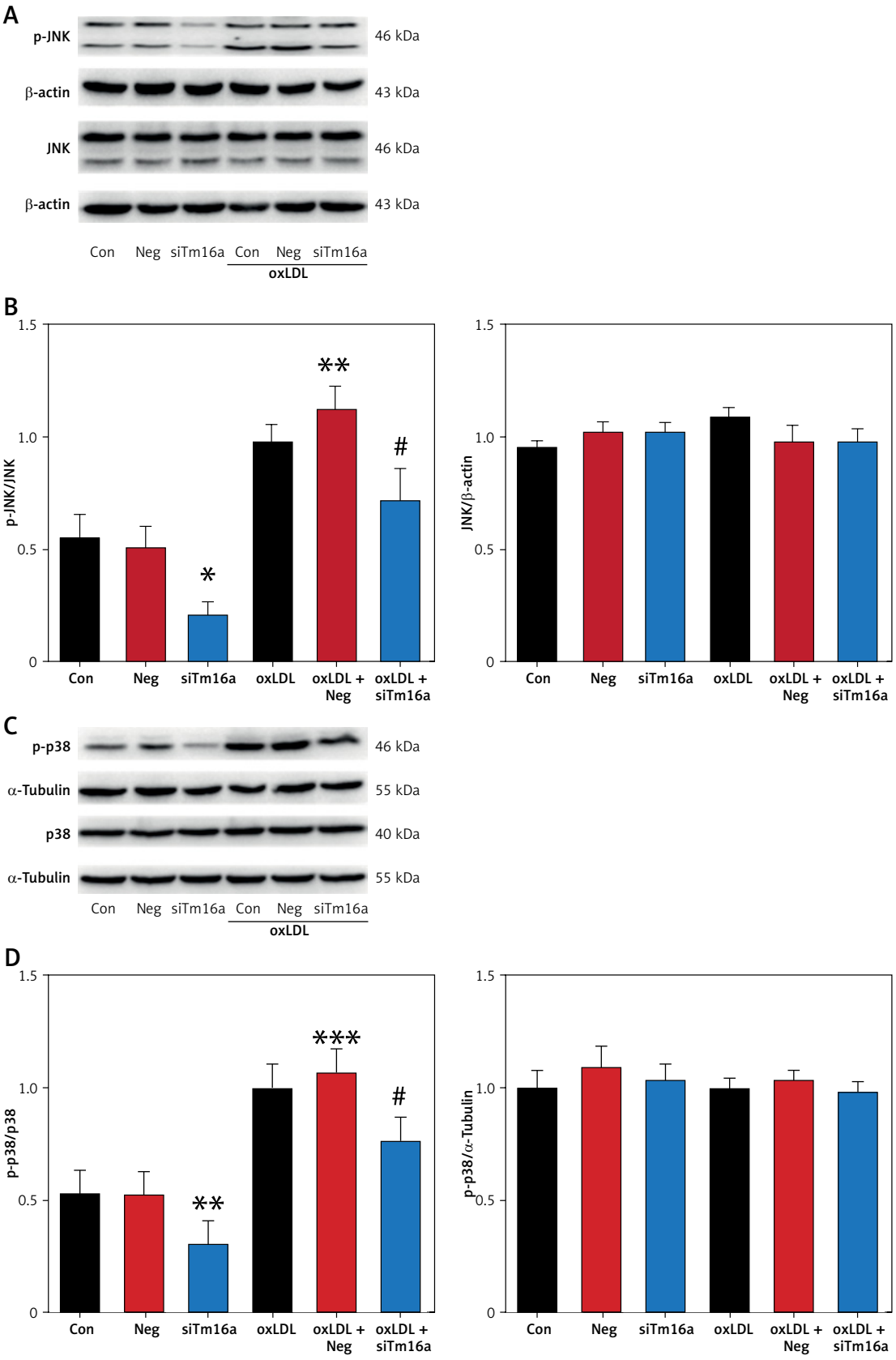

Figure 4. TMEM16A regulates expression of SR-A and CD36 through JNK/p38 pathway. **A–D** – RAW264.7 cells were transfected by TMEM16A siRNA (siRNA) with 40 nM concentration for 48 h. Then cells were treated with or without 80 μg/ml oxLDL for 24 h. Western blot was used to detect the expression of p-JNK (**A** and **B**, $n = 5$, $^{*}p < 0.05$, $^{**}p < 0.01$ vs. Neg; $^{\#}p < 0.05$ vs. oxLDL + Neg) and p-p38 (**C** and **D**, $n = 6$, $^{**}p < 0.01$, $^{***}p < 0.001$ vs. Neg; $^{\#}p < 0.05$ vs. oxLDL + Neg)

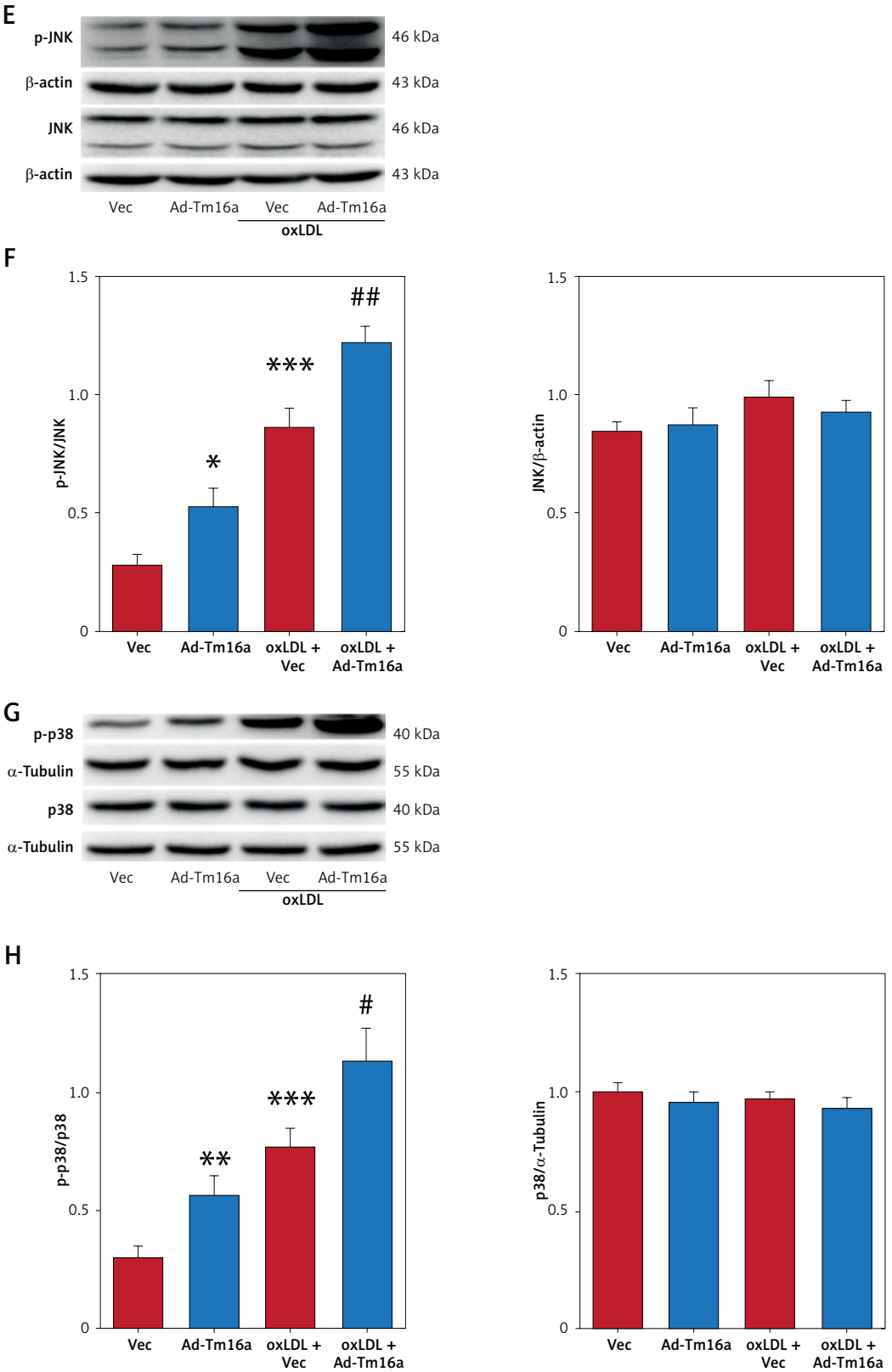

Figure 4. Cont. **E**–**H** – T RAW264.7 cells were transfected by adenovirus carrying TMEM16A cDNA (Ad-TM16A) or vector (Vec) with 100 MOI concentration for 48 h. Then cells were treated with or without 80 μg/ml oxLDL for 24 h. Western blot was used to detect the expression of p-JNK (**E**, **F**, $n = 4$, $^{*}p < 0.05$, $^{***}p < 0.001$ vs. Vec; $^{\#\#}p < 0.01$ vs. oxLDL + Vec) and p-p38 (**G**, **H**, $n = 5$, $^{**}p < 0.01$, $^{***}p < 0.001$ vs. Vec; $^{\#}p < 0.05$ vs. oxLDL + Vec)

examined the JNK and p38 MAPK pathways. JNK and p38 signaling are well known to regulate transcription factors such as AP-1 and PPARγ, which drive the expression of SR-A and CD36 [25, 26, 36, 37]. Consistent with previous findings [38, 39], our data show that TMEM16A positively regulated the phosphorylation of both kinases, whereas TMEM16A deficiency suppressed their activation.

Mechanistically, the reduction in $[Cl^-]_i$ induced by TMEM16A activation may serve as a secondary signal that triggers MAPK activation [40]. It has been shown that alterations in intracellular Cl^- concentration can affect macrophage foam cell formation [12, 19], and ClC-3 chloride channels modulate macrophage foam cell formation through regulation of $[Cl^-]_i$ [18]. However, the precise mechanism linking chloride efflux to JNK/p38 phosphorylation remains to be fully elucidated. Emerging evidence implicates chloride-sensitive kinases, particularly the With-No-Lysine (WNK) family, as critical mediators of this process. In vascular smooth muscle cells, VRCC-mediated Cl^- efflux reduces $[Cl^-]_i$ and activates WNK1, which regulates downstream proliferation pathways [41]. More directly, recent studies have established functional TMEM16A-WNK1 signaling in the vasculature: TMEM16A inhibits vascular smooth muscle cell migration in a WNK1-dependent manner [42], and endothelial TMEM16A activation reduces $[Cl^-]_i$ to stimulate WNK kinase, which in turn regulates TRPV4 channels and vasodilation [43]. Given that WNK1 is expressed in macrophages and functions as an intracellular chloride sensor regulating inflammatory responses [44], we hypothesize that macrophage TMEM16A activation reduces $[Cl^-]_i$, thereby activating WNK1 or related chloride-sensitive kinases, which subsequently phosphorylates JNK/p38 to upregulate SR-A and CD36 expression. Further investigations using WNK1-specific inhibitors or macrophage-specific

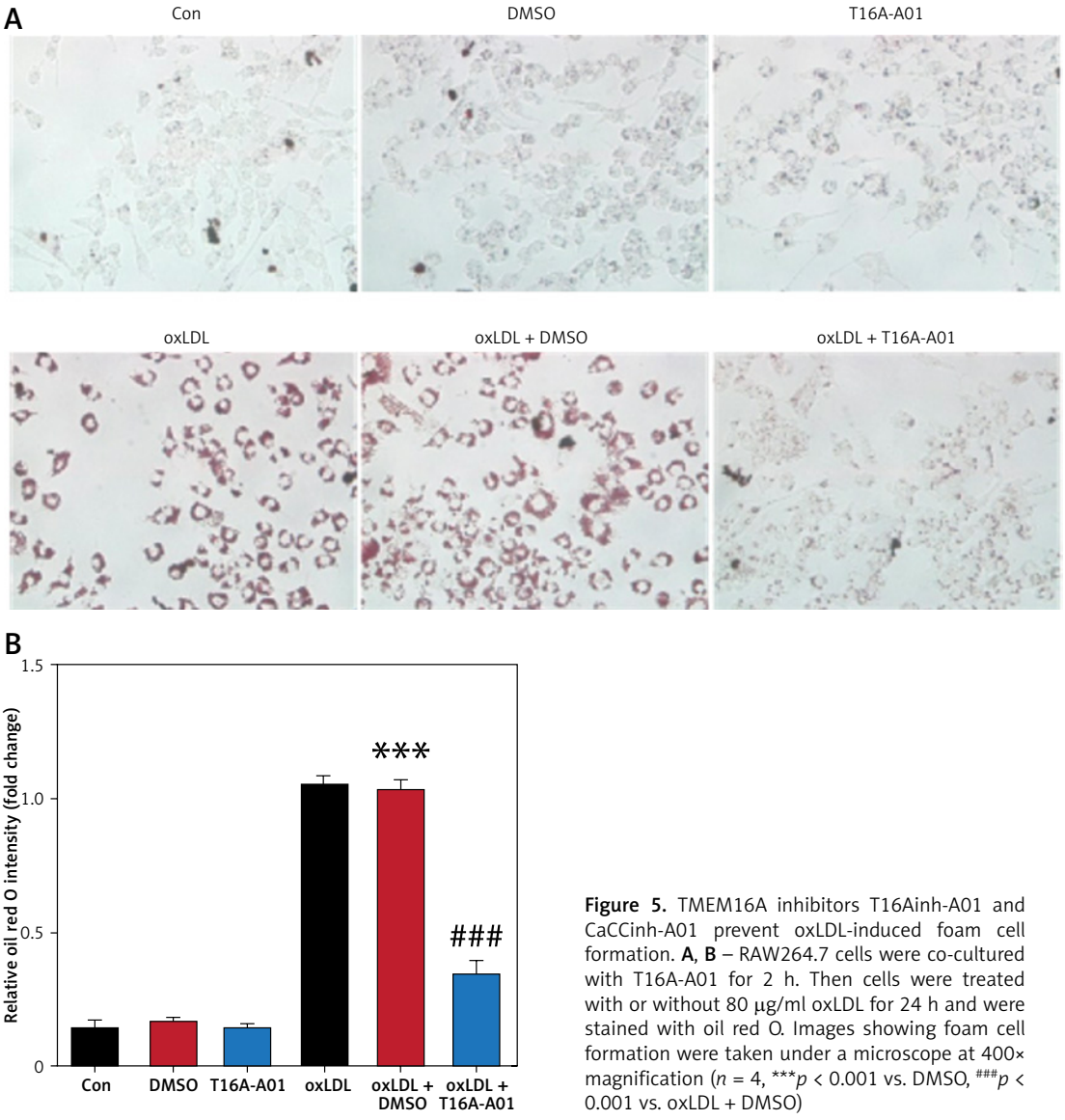

Figure 5. TMEM16A inhibitors T16Ainh-A01 and CaCCinh-A01 prevent oxLDL-induced foam cell formation. **A**, **B** – RAW264.7 cells were co-cultured with T16A-A01 for 2 h. Then cells were treated with or without 80 μg/ml oxLDL for 24 h and were stained with oil red O. Images showing foam cell formation were taken under a microscope at 400× magnification (n = 4, $^{***}p < 0.001$ vs. DMSO, $^{###}p < 0.001$ vs. oxLDL + DMSO)

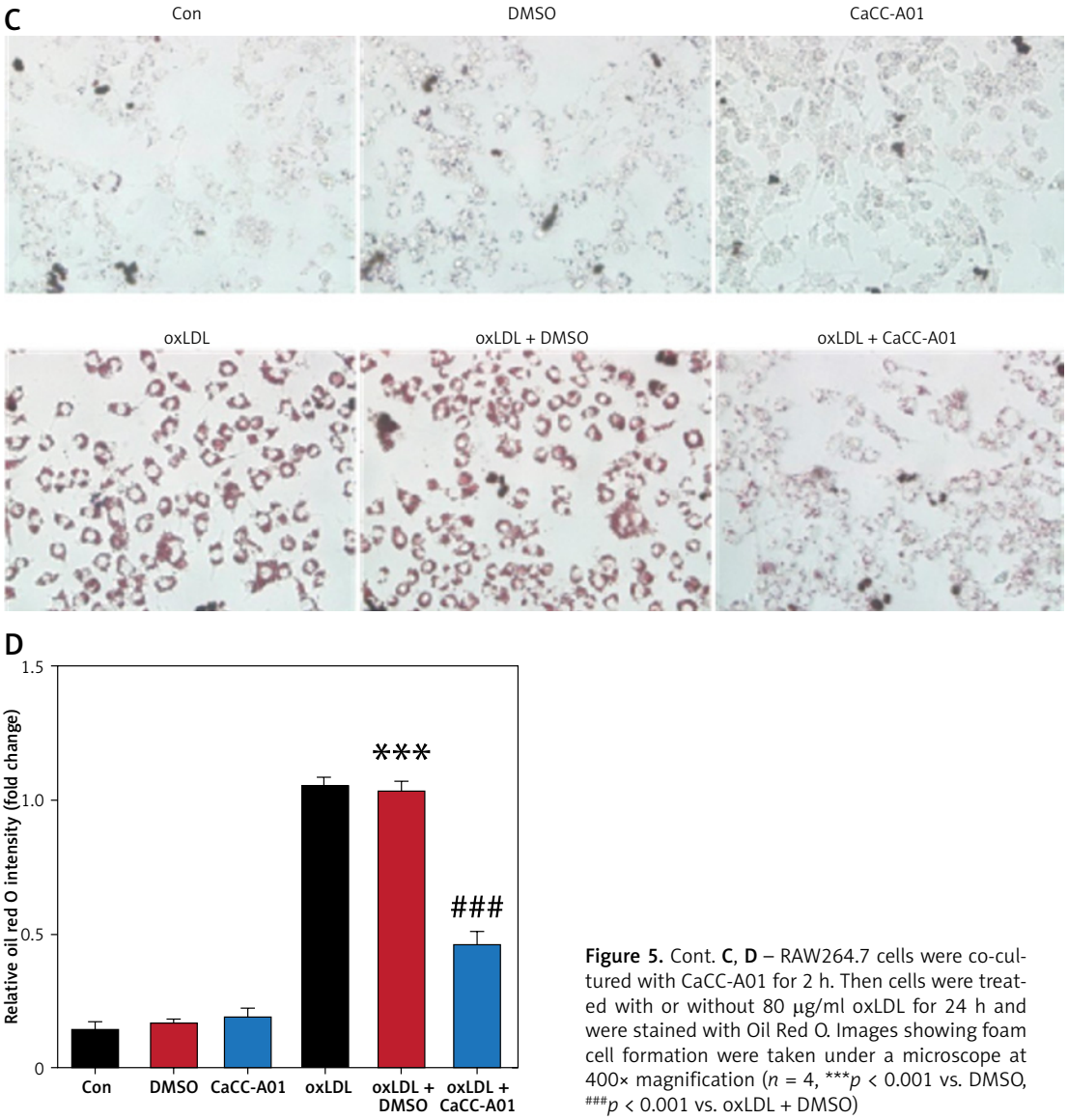

Figure 5. Cont. **C**, **D** – RAW264.7 cells were co-cultured with CaCC-A01 for 2 h. Then cells were treated with or without 80 μg/ml oxLDL for 24 h and were stained with Oil Red O. Images showing foam cell formation were taken under a microscope at 400× magnification (n = 4, $^{***}p < 0.001$ vs. DMSO, $^{###}p < 0.001$ vs. oxLDL + DMSO)

Wnk1 knockout models are warranted to verify this hypothesis. In addition to the present finding, TMEM16A has also been shown to enhance NOX2 activity and ROS production in endothelial cells [45], as well as to promote proliferation of vascular smooth muscle cells [39]. Collectively, these data raise the possibility that TMEM16A inhibition could exert multiple protective effects in the vasculature by limiting both macrophage foam cell formation and pathological vascular cell function.

The pharmacological findings in this study highlight the translational potential of targeting TMEM16A in cardiovascular therapy. We found that the TMEM16A-specific inhibitors T16Ainh-A01 [27Ano1 is expressed in all classes of ICC, including those that do not generate slow waves suggesting that Ano1 may have other functions. Indeed, a role for Ano1 in regulating proliferation of tumors and ICC has been recently suggested. Recently, a high-throughput screen identified a small molecule, T16A(inh] and CaCCinh-A01 [28] effectively mitigate macrophage lipid accumulation by suppressing the JNK/p38–SR-A/CD36 signaling pathway. Clinical studies show that benzbromarone, a well-known TMEM16A inhibitor used for gout, reduces inflammation [46] and lowers stroke risk [47, 48]. These findings suggest that, in contrast to current systemic lipid-lowering therapies, the modulation of TMEM16A may represent a novel strategy for limiting atherosclerosis.

Despite these insights, several limitations should be acknowledged. This study focused on macrophage-intrinsic mechanisms *in vitro*. Future studies employing macrophage-specific TMEM16A knockout models on ApoE-/- or Ldlr-/- backgrounds will be essential to determine whether suppression of the JNK/p38–SR-A/CD36 axis translates into reduced plaque burden and enhanced plaque stability in vivo. Moreover, while T16Ainh-A01 and CaCCinh-A01 are valuable tool

compounds, their pharmacokinetic properties, selectivity, and long-term safety profiles require further evaluation before clinical translation.

In conclusion, this study identified TMEM16A as a novel and critical regulator of macrophage foam cell formation by activating the JNK/p38 MAPK pathway and inducing the expression of scavenger receptors SR-A and CD36. These findings position TMEM16A as a promising target against atherosclerosis.

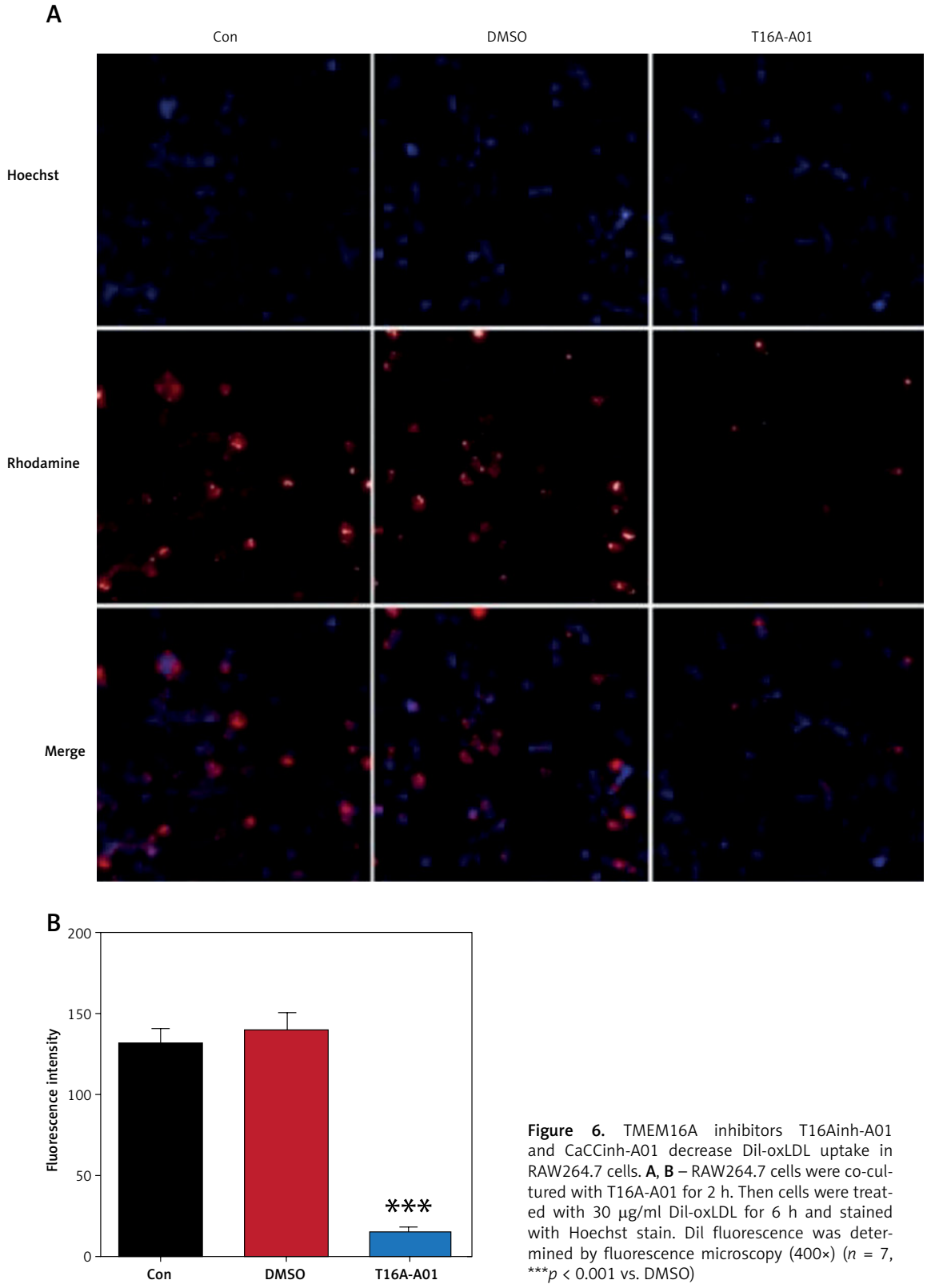

Figure 6. TMEM16A inhibitors T16Ainh-A01 and CaCCinh-A01 decrease Dil-oxLDL uptake in RAW264.7 cells. **A**, **B** – RAW264.7 cells were co-cultured with T16A-A01 for 2 h. Then cells were treated with 30 μg/ml Dil-oxLDL for 6 h and stained with Hoechst stain. Dil fluorescence was determined by fluorescence microscopy (400×) (n = 7, ***p < 0.001 vs. DMSO)

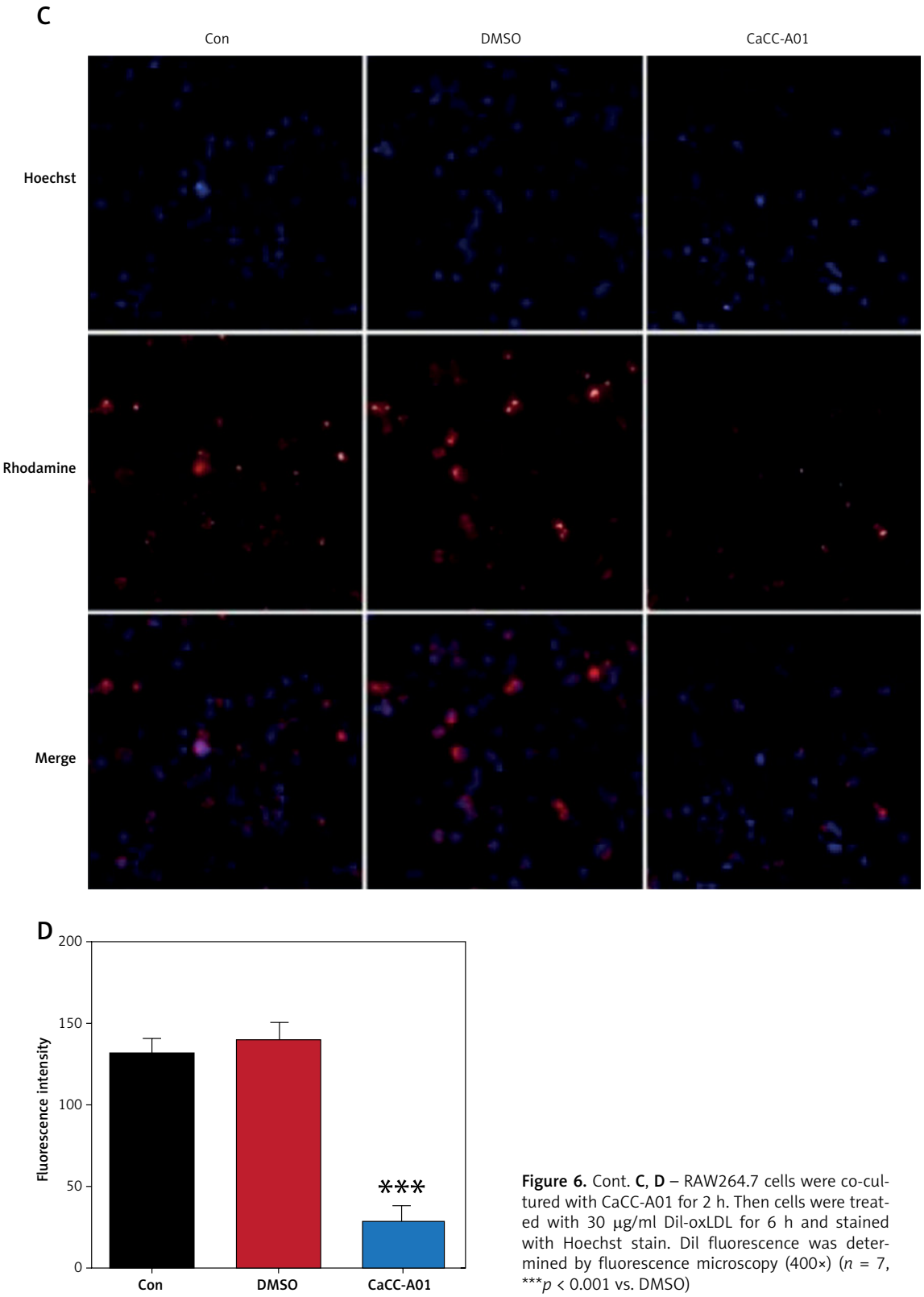

Figure 6. Cont. **C**, **D** – RAW264.7 cells were co-cultured with CaCC-A01 for 2 h. Then cells were treated with 30 μg/ml Dil-oxLDL for 6 h and stained with Hoechst stain. Dil fluorescence was determined by fluorescence microscopy (400×) (n = 7, ***p < 0.001 vs. DMSO)

Funding

This work was supported by the National Natural Science Foundation of China (No. 82470437, 82173809) and the Natural Science Foundation of Jiangsu Province (BK20250354).

Ethical approval

Not applicable.

Conflict of interest

The authors declare no conflict of interest.

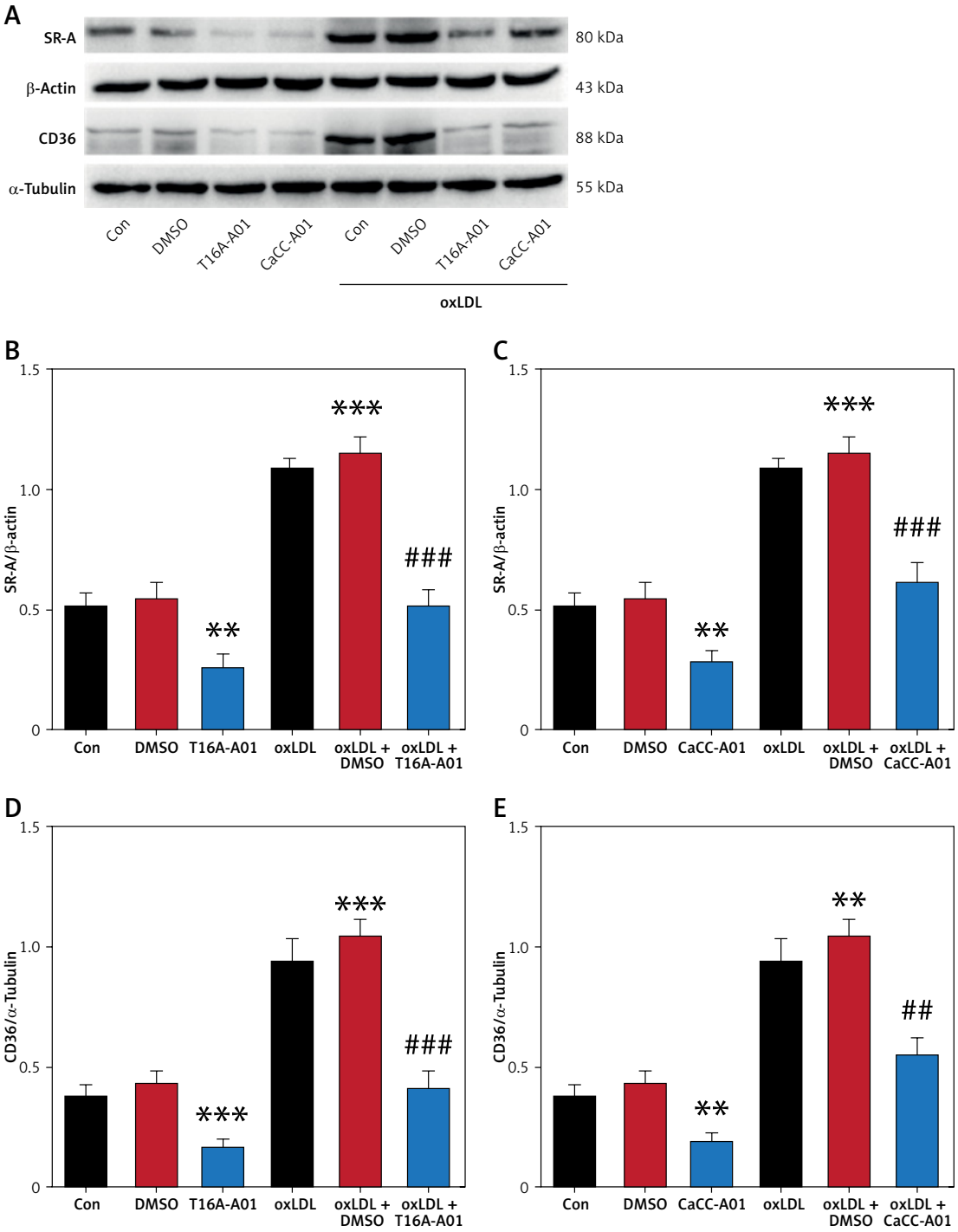

Figure 7. Pharmacological inhibition of TMEM16A blocks JNK/p38–SR-A/CD36 signaling pathway in RAW264.7 cells. **A–E** – RAW264.7 cells were co-cultured with T16Ainh-A01 or CaCCinh-A01 for 2 h. Then cells were treated with or without 80 μg/ml oxLDL for 24 h. Western blot was used to detect the expression of SR-A and CD36 (n = 5, $^{**}p < 0.01$, $^{***}p < 0.001$ vs. DMSO; $^{\#\#}p < 0.01$, $^{\#\#\#}p < 0.001$ vs. oxLDL + DMSO)

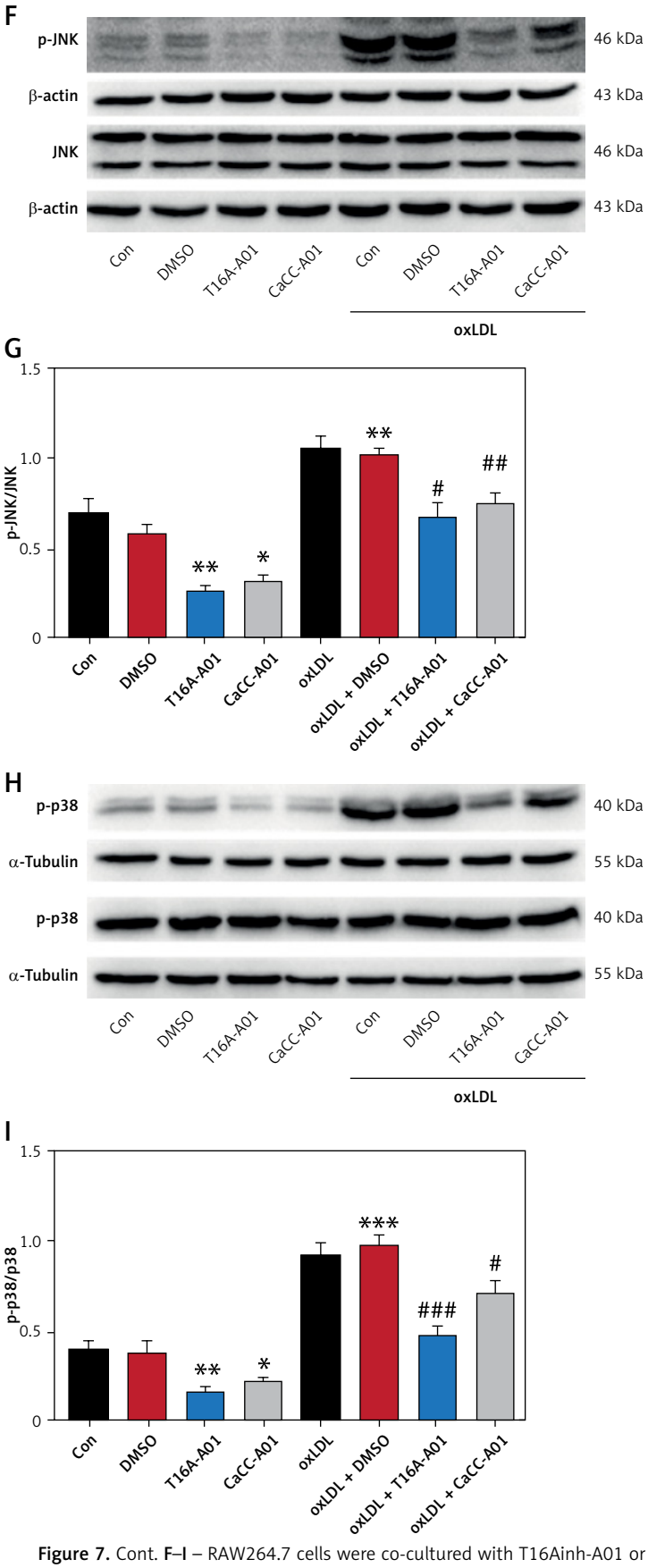

Figure 7. Cont. **F–I** – RAW264.7 cells were co-cultured with T16Ainh-A01 or CaCCinh-A01 for 2 h. Then cells were treated with or without 80 μg/ml oxLDL for 24 h. Western blot was used to detect the expression of p-JNK and p-p38 (n = 5, $^{*}p < 0.05$, $^{**}p < 0.01$, $^{***}p < 0.001$ vs. DMSO; $^{\#}p < 0.05$, $^{\#\#}p < 0.01$, $^{\#\#\#}p < 0.001$ vs. oxLDL + DMSO)

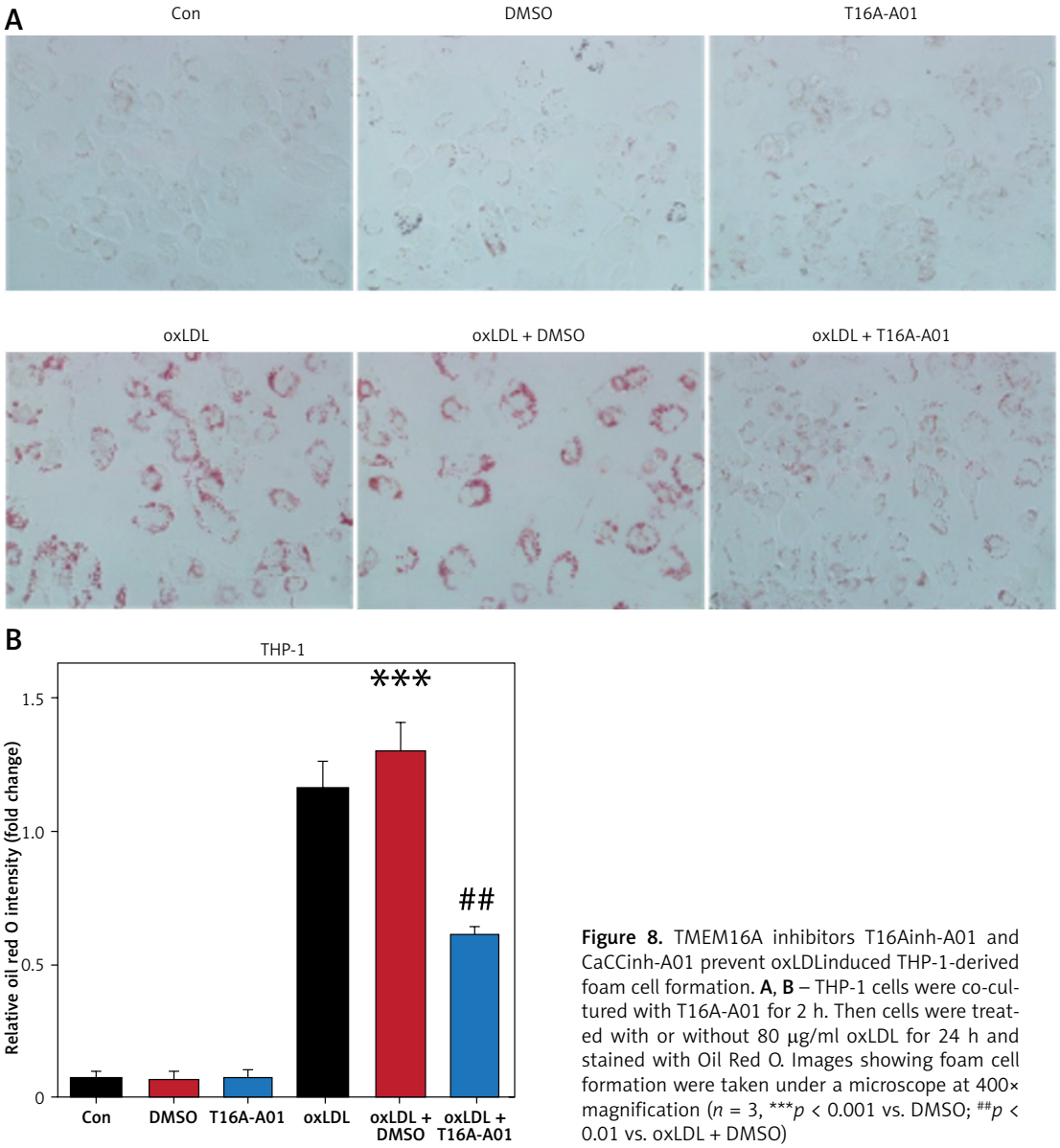

Figure 8. TMEM16A inhibitors T16Ainh-A01 and CaCCinh-A01 prevent oxLDLinduced THP-1-derived foam cell formation. **A**, **B** – THP-1 cells were co-cultured with T16A-A01 for 2 h. Then cells were treated with or without 80 μg/ml oxLDL for 24 h and stained with Oil Red O. Images showing foam cell formation were taken under a microscope at 400× magnification (n = 3, $^{***}p < 0.001$ vs. DMSO; $^{\#\#}p < 0.01$ vs. oxLDL + DMSO)

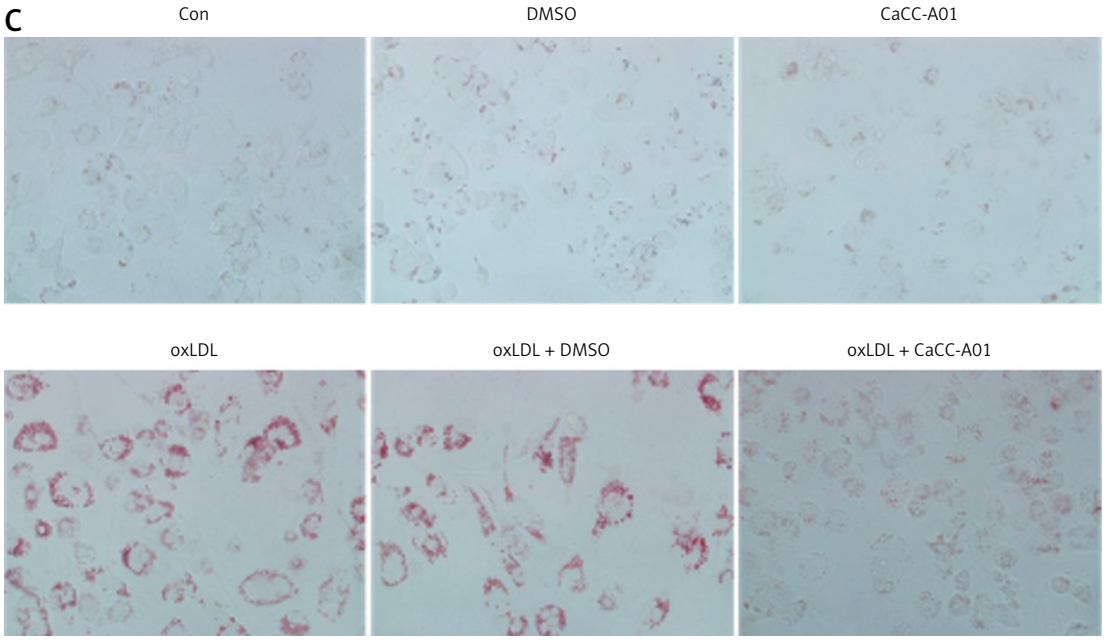

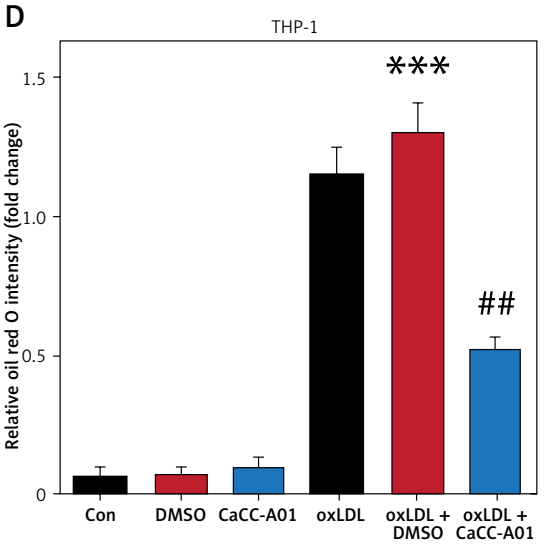

Figure 8. Cont. **C**, **D** – THP-1 cells were co-cultured with CaCC-A01 for 2 h. Then cells were treated with or without 80 μg/ml oxLDL for 24 h and stained with Oil Red O. Images showing foam cell formation were taken under a microscope at 400× magnification (n = 3, $^{***}p < 0.001$ vs. DMSO; $^{\#\#}p < 0.01$ vs. oxLDL + DMSO)

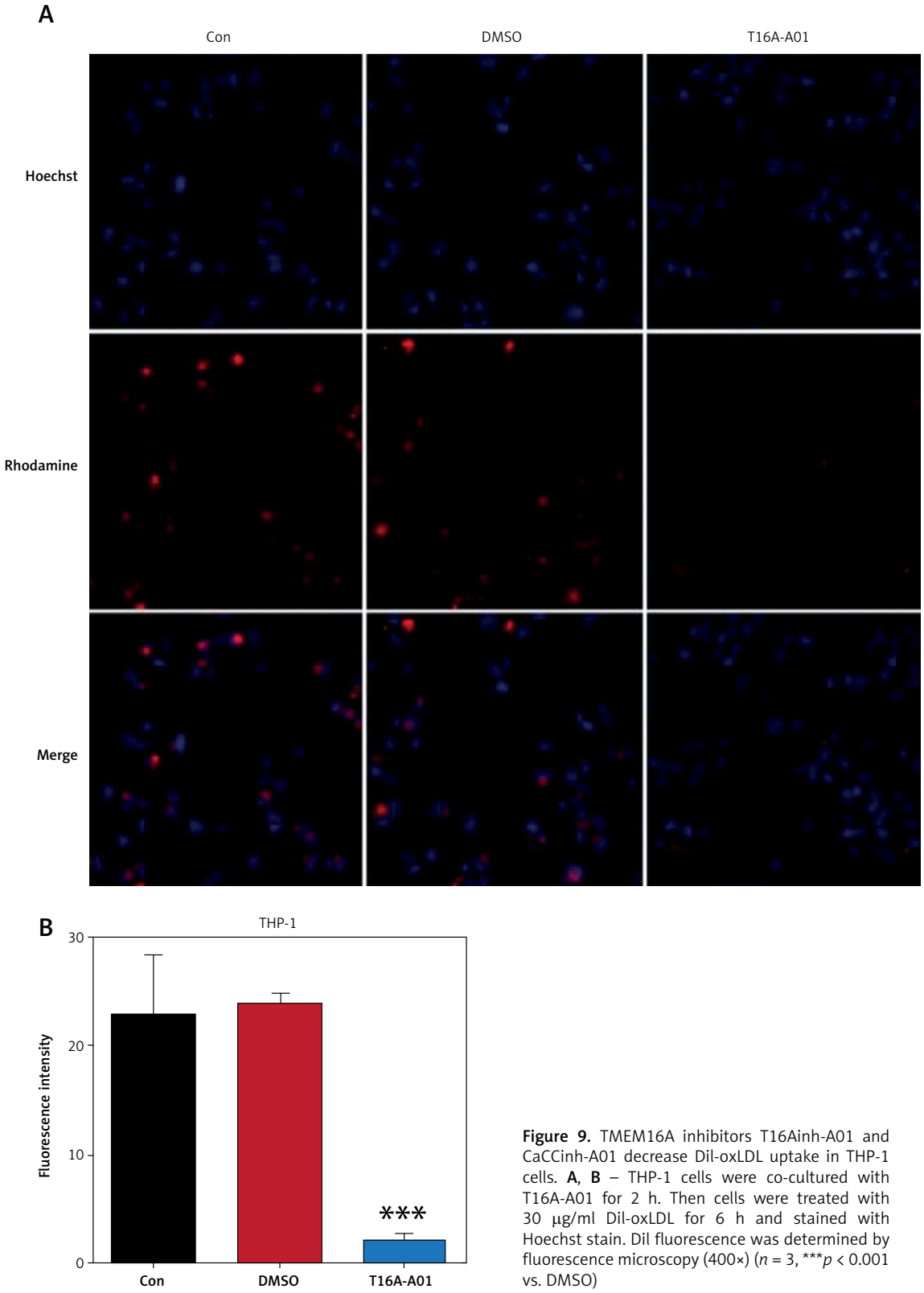

Figure 9. TMEM16A inhibitors T16Ainh-A01 and CaCCinh-A01 decrease Dil-oxLDL uptake in THP-1 cells. **A**, **B** – THP-1 cells were co-cultured with T16A-A01 for 2 h. Then cells were treated with 30 µg/ml Dil-oxLDL for 6 h and stained with Hoechst stain. Dil fluorescence was determined by fluorescence microscopy (400×) (n = 3, ***p < 0.001 vs. DMSO)

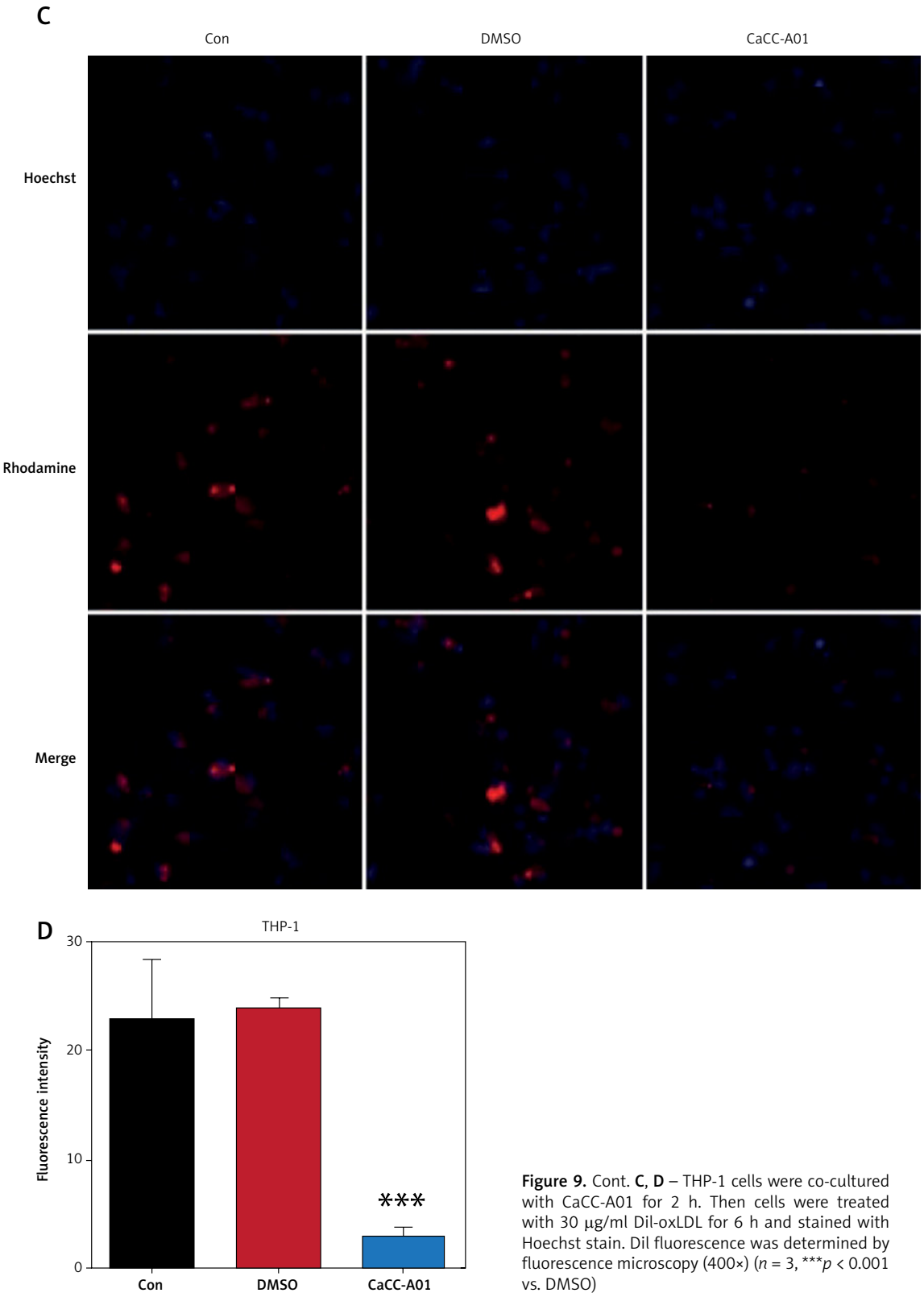

Figure 9. Cont. **C**, **D** – THP-1 cells were co-cultured with CaCC-A01 for 2 h. Then cells were treated with 30 μg/ml Dil-oxLDL for 6 h and stained with Hoechst stain. Dil fluorescence was determined by fluorescence microscopy (400×) ($n = 3$, $^{***}p < 0.001$ vs. DMSO)

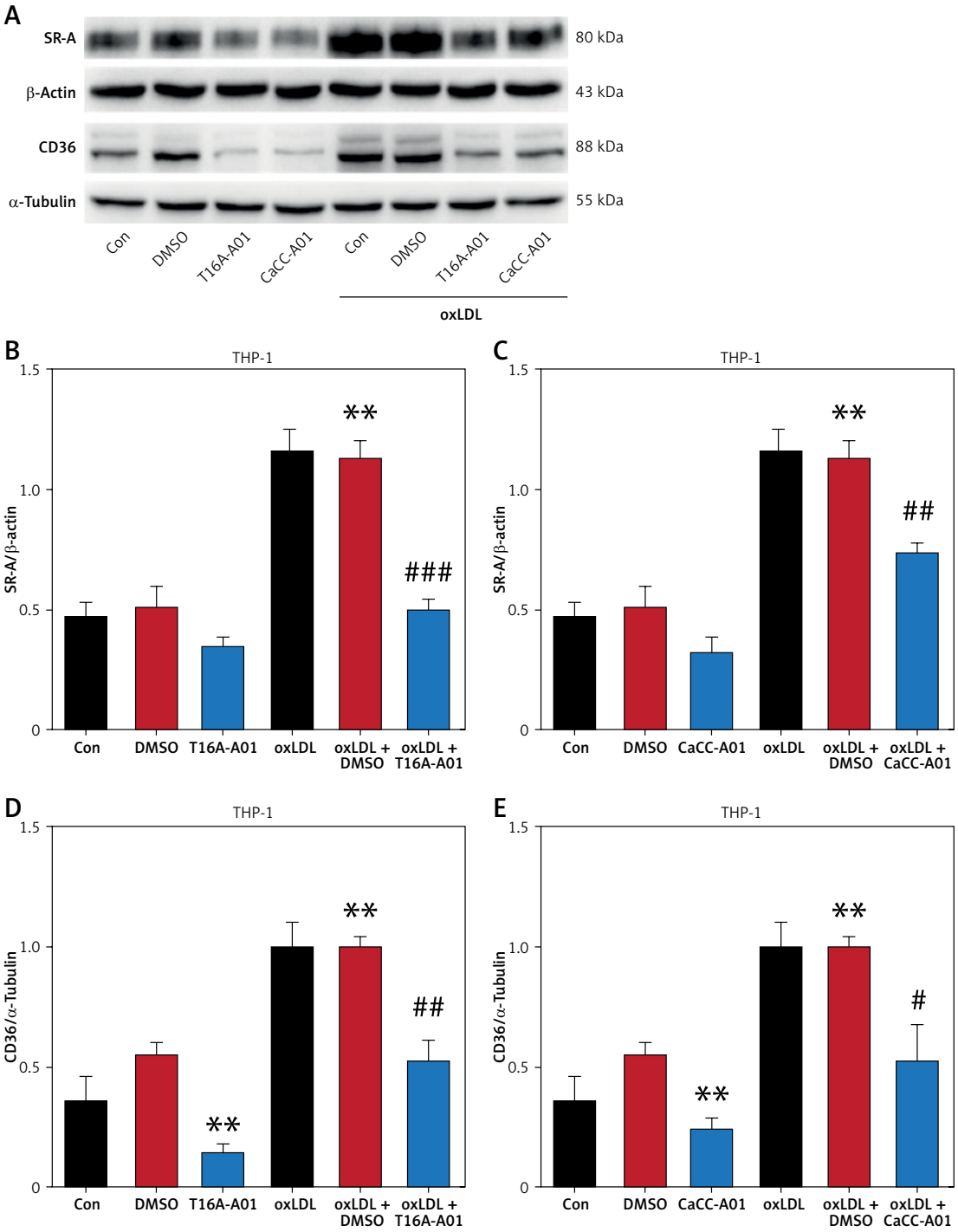

Figure 10. Pharmacological inhibition of TMEM16A blocks JNK/p38–SR-A/CD36 signaling pathway in THP-1 cells. **A–E** – THP-1 cells were co-cultured with T16Ainh-A01 or CaCCinh-A01 for 2 h. Then cells were treated with or without 80 μg/ml oxLDL for 24 h. Western blot was used to detect the expression of SR-A and CD36 (n = 3, $^{**}p < 0.01$ vs. DMSO; $^{\#}p < 0.05$, $^{\#\#}p < 0.01$, $^{\#\#\#}p < 0.001$ vs. oxLDL + DMSO)

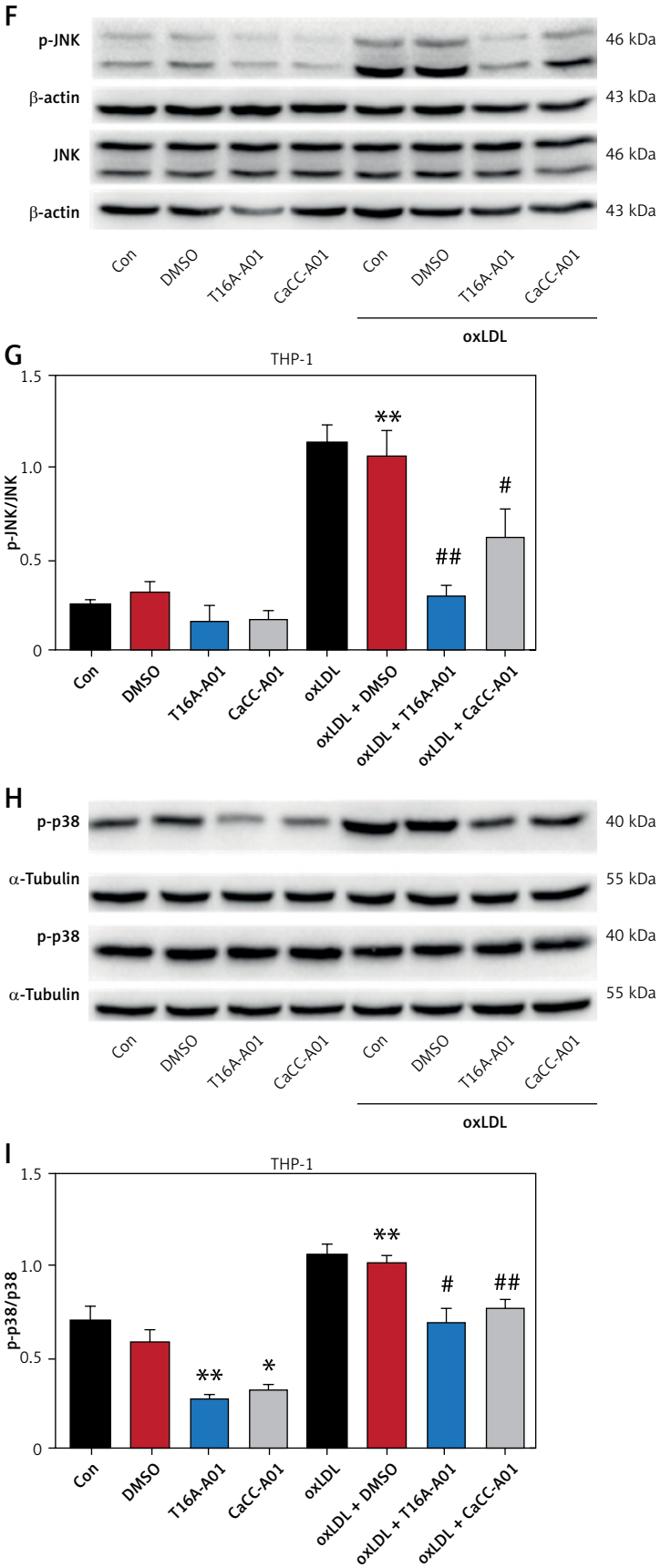

Figure 10. Cont. **F–I** – THP-1 cells were co-cultured with T16Ainh-A01 or CaCCinh-A01 for 2 h. Then cells were treated with or without 80 μg/ml oxLDL for 24 h. Western blot was used to detect the expression of p-JNK and p-p38 (n = 3, $^{*}p < 0.05$, $^{**}p < 0.01$ vs. DMSO; $^{\#}p < 0.05$, $^{\#\#}p < 0.01$ vs. oxLDL + DMSO)

References

1. Sarraju A, Nissen SE. Atherosclerotic plaque stabilization and regression: a review of clinical evidence. Nat Rev Cardiol 2024; 21: 487-97.
2. Banach M, Surma S, Toth PP. 2023: The year in cardiovascular disease – the year of new and prospective lipid lowering therapies. Can we render dyslipidemia a rare disease by 2024? Arch Med Sci 2023; 19: 1602-15.
3. Takaoka M, Zhao X, Lim HY, et al. Early intermittent hyperlipidaemia alters tissue macrophages to fuel atherosclerosis. Nature 2024; 634: 457-65.
4. Ai J, Tang X, Zhou Y, et al. New insights into foam cells in atherosclerosis. Cardiovasc Res 2025; 121: 2334-46.
5. Mukherjee P, Rahaman SG, Goswami R, et al. Role of mechanosensitive channels/receptors in atherosclerosis. Am J Physiol Cell Physiol 2022; 322: C927-38.
6. Lan Y, Lu J, Zhang S, et al. Piezo1-mediated mechanotransduction contributes to disturbed flow-induced atherosclerotic endothelial inflammation. J Am Heart Assoc 2024; 13: e035558.
7. Atcha H, Kulkarni D, Meli VS, et al. Piezo1-mediated mechanotransduction enhances macrophage oxidized low-density lipoprotein uptake and atherogenesis. PNAS Nexus 2024; 3: pgae436.
8. Zhang Y, Ma K, Fang X, et al. Targeting ion homeostasis in metabolic diseases: Molecular mechanisms and targeted therapies. Pharmacol Res 2025; 212: 107579.
9. Azlan NFM, Zhang J. Role of the cation-chloride-cotransporters in cardiovascular disease. Cells 2020; 9: 2293.
10. Wang M, Yang H, Zheng LY, et al. Downregulation of TMEM16A calcium-activated chloride channel contributes to cerebrovascular remodeling during hypertension by promoting basilar smooth muscle cell proliferation. Circulation 2012; 125: 697-707.
11. Raut SK, Singh K, Sanghvi S, et al. Chloride ions in health and disease. Biosci Rep 2024; 44: BSR20240029.
12. Wu QQ, Liu XY, Xiong LX, et al. Reduction of intracellular chloride concentration promotes foam cell formation. Circ J 2016; 80: 1024-33.
13. Li X, Du YX, Yu CL, Niu N. Ion channels in macrophages: implications for disease progression. Int Immunopharmacol 2025; 144: 113628.
14. Zeng XL, Sun L, Zheng HQ, et al. Smooth muscle-specific TMEM16A expression protects against angiotensin II-induced cerebrovascular remodeling via suppressing extracellular matrix deposition. J Mol Cell Cardiol 2019; 134: 131-43.
15. Al-Hosni R, Kaye R, Choi CS, Tammaro P. The TMEM16A channel as a potential therapeutic target in vascular disease. Curr Opin Nephrol Hypertens 2024; 33: 161-9.
16. Zhang X, Zheng B, Yang Z, et al. TMEM16A and myocardin form a positive feedback loop that is disrupted by KLF5 during Ang II–induced vascular remodeling. Hypertension 2015; 66: 412-21.
17. Lv XF, Zhang YJ, Liu X, et al. TMEM16A ameliorates vascular remodeling by suppressing autophagy via inhibiting Bcl-2-p62 complex formation. Theranostics 2020; 10: 3980-93.
18. Tao J, Liu CZ, Yang J, et al. ClC-3 deficiency prevents atherosclerotic lesion development in ApoE-/- mice. J Mol Cell Cardiol 2015; 87: 237-47.
19. Hong L, Xie ZZ, Du YH, et al. Alteration of volume-regulated chloride channel during macrophage-derived foam cell formation in atherosclerosis. Atherosclerosis 2011; 216: 59-66.
20. Genovese M, Buccirossi M, Guidone D, et al. Analysis of inhibitors of the anoctamin-1 chloride channel (transmembrane member 16A, TMEM16A) reveals indirect mechanisms involving alterations in calcium signalling. Br J Pharmacol 2023; 180: 775-85.
21. Bradley E, Fedigan S, Webb T, et al. Pharmacological characterization of TMEM16A currents. Channels 2014; 8: 308-20.
22. Dejager S, Mietus-Synder M, Pitas RE. Oxidized low density lipoproteins bind to the scavenger receptor expressed by rabbit smooth muscle cells and macrophages. Arterioscler Thromb 1993; 13: 371-8.
23. Lian TW, Wang L, Lo YH, Huang IJ, Wu MJ. Fisetin, morin and myricetin attenuate CD36 expression and oxLDL uptake in U937-derived macrophages. Biochim Biophys Acta 2008; 1781: 601-9.
24. Kunjathoor VV, Febbraio M, Podrez EA, et al. Scavenger receptors class A-I/II and CD36 are the principal receptors responsible for the uptake of modified low density lipoprotein leading to lipid loading in macrophages. J Biol Chem 2002; 277: 49982-8.
25. Liu Q, Fan J, Bai J, et al. IL-34 promotes foam cell formation by enhancing CD36 expression through p38 MAPK pathway. Sci Rep 2018; 8: 17347.
26. Yin R, Dong Y, Li H. PPARγ phosphorylation mediated by JNK MAPK: a potential role in macrophage-derived foam cell formation. Acta Pharmacol Sin 2006; 27: 1146-52.
27. Mazzone A, Eisenman ST, Strege PR, et al. Inhibition of cell proliferation by a selective inhibitor of the Ca(2+)-activated Cl(-) channel, Ano1. Biochem Biophys Res Commun 2012; 427: 248-53.
28. Bill A, Hall ML, Borawski J, et al. Small molecule-facilitated degradation of ANO1 protein: a new targeting approach for anticancer therapeutics. J Biol Chem 2014; 289: 11029-41.
29. Weir HK, Anderson RN, Coleman King SM, et al. Heart disease and cancer deaths – trends and projections in the United States, 1969–2020. Prev Chronic Dis 2016; 13: E157.
30. Ceasovschih A, Banjanin N, Bednarek A, et al. Atherosclerotic features in patients with heart failure. Arch Med Sci 2025; 21: 1107-29.
31. Toth PP, Banach M. 2025: The year in cardiovascular disease – the year of triglyceride lowering therapies. Can we effectively reduce triglyceride-related residual cardiovascular disease and pancreatitis risk? Arch Med Sci 2025; 21: 2229-45.
32. Tabas I, Bornfeldt KE. Macrophage phenotype and function in different stages of atherosclerosis. Circ Res 2016; 118: 653-67.
33. Takaoka M, Zhao X, Lim HY, et al. Early intermittent hyperlipidaemia alters tissue macrophages to fuel atherosclerosis. Nature 2024; 634: 457-65.
34. Duan DD. The ClC-3 chloride channels in cardiovascular disease. Acta Pharmacol Sin 2011; 32: 675-84.
35. Goto K, Kitazono T. Chloride ions, vascular function and hypertension. Biomedicines 2022; 10: 2316.
36. Oh J, Riek AE, Weng S, et al. Endoplasmic reticulum stress controls M2 macrophage differentiation and foam cell formation. J Biol Chem 2012; 287: 11629-41.
37. Ricote M, Li AC, Willson TM, Kelly CJ, Glass C K. The peroxisome proliferator-activated receptor-γ is a negative regulator of macrophage activation. Nature 1998; 391: 79-82.
38. Allawzi AM, Vang A, Clements RT, et al. Activation of anoctamin-1 limits pulmonary endothelial cell proliferation via p38–mitogen-activated protein kinase–dependent apoptosis. Am J Respir Cell Mol Biol 2018; 58: 658-67.

39. Liu D, Wang K, Su D, et al. TMEM16A regulates pulmonary arterial smooth muscle cells proliferation via p38MAPK/ERK pathway in high pulmonary blood flow-induced pulmonary arterial hypertension. J Vasc Res 2020; 58: 27-37.
40. Sun W, Guo S, Li Y, et al. Anoctamin 1 controls bone resorption by coupling Cl- channel activation with RANKL-RANK signaling transduction. Nat Commun 2022; 13: 2899.
41. Zhang Y, Zheng HQ, Chen BY, et al. WNK1 is required for proliferation induced by hypotonic challenge in rat vascular smooth muscle cells. Acta Pharmacol Sin 2018; 39: 35-47.
42. Zheng H, Li X, Zeng X, et al. TMEM16A inhibits angiotensin II-induced basilar artery smooth muscle cell migration in a WNK1-dependent manner. Acta Pharm Sin B 2021; 11: 3994-4007.
43. Garrud TAC, Bell B, Mata-Daboin A, et al. WNK kinase is a vasoactive chloride sensor in endothelial cells. Proc Natl Acad Sci USA 2024; 121: e2322135121.
44. Mayes-Hopfinger L, Enache A, Xie J, et al. Chloride sensing by WNK1 regulates NLRP3 inflammasome activation and pyroptosis. Nat Commun 2021; 12: 4546.
45. Ma MM, Gao M, Guo KM, et al. TMEM16A contributes to endothelial dysfunction by facilitating Nox2 NADPH oxidase–derived reactive oxygen species generation in hypertension. Hypertension 2017; 69: 892-901.
46. Kimura Y, Yanagida T, Onda A, et al. Soluble uric acid promotes atherosclerosis via AMPK (AMP-activated protein kinase)-mediated inflammation. Arterioscler Thromb Vasc Biol 2020; 40: 570-82.
47. Niu SW, Hung CC, Lin HYH, et al. Reduced incidence of stroke in patients with gout using benzbromarone. J Pers Med 2022; 12: 28.
48. Al-Hosni R, Ilkan Z, Agostinelli E, Tammaro P. The pharmacology of the TMEM16A channel: therapeutic opportunities. Trends Pharm Sci 2022; 43: 712-25.